Applied Energy 122 (2014) 288–309

Contents lists available at ScienceDirect

Applied Energy

journal homepage: www.elsevier.com/locate/apenergy

A UK-based assessment of hybrid PV and solar-thermal systems for domestic heating and power: System performance

María Herrando, Christos N. Markides *, Klaus Hellgardt

Department of Chemical Engineering, Imperial College London, London SW7 2AZ, UK

HIGHLIGHTS

- We develop a mathematical model to simulate a hybrid solar-thermal system (PVT).
- Household electricity and hot water demands covered throughout a year are estimated.
- Two key system parameters are varied to optimise the system performance.
- Up to 51% of the annual electrical and 36% of the hot water demands are covered.
- In addition, 16.0 tCO_2 (35% higher than PV-only) are saved over a 20-year lifetime.

ARTICLE INFO

Article history:
Received 7 May 2013
Received in revised form 25 January 2014
Accepted 29 January 2014
Available online 12 March 2014

Keywords:
Hybrid PV
Domestic UK energy demand
Heat and power provision
Solar energy
System performance

ABSTRACT

The goal of this paper is to assess the suitability of hybrid PVT systems for the provision of electricity and hot water (space heating is not considered) in the UK domestic sector, with particular focus on a typical terraced house in London. A model is developed to estimate the performance of such a system. The model allows various design parameters of the PVT unit to be varied, so that their influence in the overall system performance can be studied. Two key parameters, specifically the covering factor of the solar collector with PV and the collector flow-rate, are considered. The emissions of the PVT system are compared with those incurred by a household that utilises a conventional energy provision arrangement. The results show that for the case of the UK (low solar irradiance and low ambient temperatures) a complete coverage of the solar collector with PV together with a low collector flow-rate are beneficial in allowing the system to achieve a high coverage of the total annual energy (heat and power) demand, while maximising the CO_2 emissions savings. It is found that with a completely covered collector and a flow-rate of 20 L/h, 51% of the total electricity demand and 36% of the total hot water demand over a year can be covered by a hybrid PVT system. The electricity demand coverage value is slightly higher than the PV-only system equivalent (49%). In addition, our emissions assessment indicates that a PVT system can save up to 16.0 tonnes of CO_2 over a lifetime of 20 years, which is significantly (36%) higher than the 11.8 tonnes of CO_2 saved with a PV-only system. All investigated PVT configurations outperformed the PV-only system in terms of emissions. Therefore, it is concluded that hybrid PVT systems offer a notably improved proposition over PV-only systems.

1. Introduction

A significant increase in energy demand has been observed in the last decades, driven by an increase in population and/or in the energy use per capita in various regions around the globe. In the UK, energy use per capita has actually decreased by about 15% since its peak in the late 1990s, which has more than compensated for the ~10% increase in population over the same period [1]. There is a significant and continuing desire to maintain this trend, and to diversify and decarbonise the energy supply, thus lowering the reliance on fossil fuels, which arises from the realisation that these are finite resources (giving rise to economic, security of supply and sustainability concerns) and also that the emissions associated with their use lead to wider environmental and health problems [1]. Specifically, the UK has made a number of international commitments and set itself a series of targets for reducing greenhouse gas emissions and increasing the proportion of final energy supplied by renewable sources [2].

* Corresponding author. Tel.: +44 20 759 41601.
E-mail address: c.markides@imperial.ac.uk (C.N. Markides).

http://dx.doi.org/10.1016/j.apenergy.2014.01.061
0306-2619

Nomenclature

Abbreviations

a-Si	amorphous-crystalline PV module
c-Si	mono-crystalline PV module
pc-Si	poly-crystalline PV module
MPP	Maximum Power Point
NOCT	Normal Operating Cell Temperature
PV	photovoltaic
PVT	PV and solar-thermal system
PVT/w	PV and solar-thermal water system

Symbols

A_c	collector aperture area (m^2)
A_{PV}	surface area of the PV (m^2)
c_p	specific heat capacity of water (=4180 J/kg K)
D	diameter of the riser tubes (m)
DC_{av}	percentage of the average overall demand covered by the PVT system (%)
DC_E	percentage of the electricity demand covered by the PVT system (%)
DC_{HW}	percentage of the hot water demand covered by the PVT system (%)
DC_{wav}	percentage of the weighted average overall demand covered by the PVT system (%)
e_{ag}	thickness of the air gap (m)
e_i	thickness of the insulation layer (m)
E_{grid}	electrical energy required from the grid over a full year (kW_e h)
E_{loss}	electrical energy consumed by the water pump (kW_e h)
E_{net}	additional (to the PVT-generated) electrical energy required to cover the short-fall in the household demand over a full year (kW_e h)
E_{neti}	additional (to the PVT-generated) electrical energy required to cover the short-fall in the household demand at time step i (W_e h)
E_{PV}	electrical energy produced by the PV-only system over a full year (kW_e h)
E_{PVT}	electrical energy produced by the PVT system over a full year (kW_e h)
E_{PVTi}	Electrical energy produced by the PVT system at time step i (W_e h)
E_{PVTnet}	net electrical energy available from the household after subtraction of the household's consumption over a full year (kW_e h)
E_T	total annual electricity demand (kW_e h)
E_{wd}, E_{we}	electricity consumption over a day, either during the week or on the weekend respectively (kW_e h)
Em_{aux}	total CO_2 (equivalent) emissions due to the auxiliary heater over a full year (kg CO_2(e))
Em_{cE}	total CO_2 (equivalent) emissions from covering the total electricity demand from the grid over a full year (kg CO_2(e))
Em_{cHW}	total CO_2 (equivalent) emissions from covering the overall hot water demand with an equivalent conventional system (natural gas boiler, heat pump or electrical heater) over a full year (kg CO_2(e))
Em_{PVTE}	total CO_2 (equivalent) emissions incurred to cover the demand with an installed PVT unit over a full year (kg CO_2(e))
Em_{sE}	percentage of CO_2 (equivalent) emission savings due to the electricity demand covered by the PVT system (%)
Em_{sHW}	percentage of CO_2 (equivalent) emission savings due to hot water production by the PVT system (%)
Em_{sT}	total CO_2 (equivalent) emissions saved over a full year when PVT systems are used to cover the demand (kg CO_2(e)/year)
f	Darcy–Weisbach (or Moody) friction factor for the water flow through the pipes
g	gravitational acceleration (=9.81 m/s^2)
G_{bi}	thermal conductance between the absorber, the back/underside insulation and the environment (W/m^2 K)
G_{ca}	thermal conductance between the PV laminate layer and the absorber plate (W/m^2 K)
Gr	Grashof number
h_{air}	free convective heat transfer coefficient of air at the back/underside of the PVT module (W/m^2 K)
h_w	convective heat transfer coefficient of the water flow in the pipes (W/m^2 K)
h_{wind}	convective heat transfer coefficient due to wind flow over the PVT (W/m^2 K)
J	incident global solar irradiance on the tilted PVT collector surface (W/m^2)
k_{air}	thermal conductivity of air (W/m K)
k_i	thermal conductivity of the insulation layer (W/m K)
k_w	thermal conductivity of water (W/m K)
K_s	minor loss coefficient for flow through a bend
L	total length of the water pipe (m)
$\dot{m}_c$	mass flow-rate of water through the collector (kg/s)
$\dot{m}_l$	mass flow-rate of hot water demand (kg/s)
$\dot{m}_t$	mass flow-rate of water through the heat-exchanger located in the hot water tank (kg/s)
$\dot{m}_{tube}$	mass flow-rate of water flowing through the riser tubes of the collector (kg/s)
M_t	total mass of water in the hot water tank (kg)
NTU	Number of Transfer Units
Nu	Nusselt number
P	PV area covering factor (%)
P_{net}	net electrical power output of the PVT system (W)
P_{PV}	electrical power output of the PV module (W)
P_P	electrical power consumed by the water pump (W)
P_{wd}, P_{we}	electrical power demand at a specific time of the day, either during the week or on the weekend (W)
$\dot{q}_{ag}$	heat flux from the glass cover to the PV laminate layer due to both conduction and convection through the air gap (W/m^2)
$\dot{q}_{agab}$	heat flux from the glass cover to the absorber plate due to convection through the air gap in the uncovered section without PV (W/m^2)
$\dot{q}_{aux}$	auxiliary heater power (W)
$\dot{q}_{bi}$	heat flux through the back/underside insulation (W/m^2)
$\dot{q}_{biab}$	heat flux through the back/underside insulation in the uncovered section without PV (W/m^2)
$\dot{q}_{ca}$	heat flux from the PV laminate to the absorber (W/m^2)
$\dot{q}_{caab}$	heat flux through the absorber plate in the uncovered section without PV (W/m^2)
$\dot{q}_{ct}$	heat addition from the collector to the hot water tank (W)
$\dot{q}_{loss}$	heat losses through the hot water tank walls (W)
$\dot{q}_{load}$	heat removal to cover the domestic hot water demand (W)
$\dot{q}_{rPV}$	heat flux from the glass cover to the PV laminate due to radiation (W/m^2)
$\dot{q}_{rab}$	heat flux from the glass cover to the absorber plate due to radiation (W/m^2)
$\dot{q}_{sky}$	heat flux loss between the glass cover and the sky due to radiation (W/m^2)
$\dot{q}_{skya}$	heat flux loss from the glass cover to the sky in the uncovered section without PV due to radiation (W/m^2)
$\dot{q}_w$	heat flux transferred from the absorber to the water (W/m^2)

$\dot{q}_{wab}$	heat flux transferred from the absorber plate to the water in the uncovered section without PV (W/m^2)
$\dot{q}_{wind}$	heat flux loss due to wind forced convection (W/m^2)
$\dot{q}_{winda}$	heat flux loss due to wind forced convection in the uncovered section without PV (W/m^2)
Q	total collector water flow-rate (m^3/s)
Q_{aux}	total auxiliary heating required over a full year (kW$_{th}$ h)
Q_{gas}	additional amount of heat required (kW$_{th}$ h)
Q_{PVT}	amount of hot water produced by the PVT system over a full year (kW$_{th}$ h)
Q_T	total hot water household demand over a full year (kW$_{th}$ h)
R_{EVA}	heat resistance of the EVA layer (m^2 K/W)
R_{glue}	heat resistance of the glue layer (m^2 K/W)
R_{ted}	heat resistance of the Tedlar layer (m^2 K/W)
R_i	heat resistance of the insulation layer (m^2 K/W)
R_{air}	heat resistance of the air layer (m^2 K/W)
Re	Reynolds number
S_t	surface area of the hot water tank (m^2)
T_∞	free-stream temperature (K)
T_a	ambient temperature (K)
T_{as}	ambient temperature surrounding the hot water tank (K)
T_{ab}	temperature of the absorber plate (K)
T_{aba}	temperature at the front/top surface of the absorber plate in the uncovered section without PV (K)
T_{abf}	temperature at the bottom surface of the absorber plate in the uncovered section without PV (K)
T_{bw}	bulk temperature of the water in the collector (K)
T_{bwab}	bulk temperature of the water in the uncovered section without PV (K)
T_{cin}	temperature of the water entering the collector (K)
T_{cout}	temperature of the water exiting the collector (K)
T_{del}	delivery temperature of hot water to the household (K)
T_g	temperature of the glass cover (K)
T_{ga}	temperature of the glass cover in the section that is not covered by PV and open to the atmosphere (K)
T_{PVref}	reference PV cell temperature at an ambient temperature of T_a = 25 °C and a solar irradiance of J = 1000 W/m^2 (K)
T_{PV}	PV cell temperature (K)
T_{PVmax}	maximum PV cell temperature reached in a day (K)
T_{PVout}	temperature of the water entering the uncovered section without PV (K)
T_s	surface temperature (K)
T_{sky}	sky temperature (K)
T_{sup}	mains water supply temperature (K)
T_t	temperature of the water in the hot water tank (K)
T_{tin}	temperature of the collector flow at the inlet of the heat exchanger immersed in the hot water tank (K)
T_{tout}	temperature of the collector flow at the outlet of the heat exchanger immersed in the hot water tank (K)
T_{win}	temperature of the water entering the hot water tank (K)
U_t	overall heat loss coefficient of the hot water tank (W/m^2 K)
$(UA)_t$	overall heat transfer coefficient-area product of the heat exchanger located inside the hot water tank (W/K)
V_P	water flow-rate through the collector (with 1 L/h = 2.78 × 10^{-7} m^3/s)
v_{wind}	wind speed (m/s)
v_w	bulk water flow speed in the pipes (m/s)

Greek

α_{ab}	absorptivity of the absorber plate
α_{PV}	absorptivity of the PV module
β_0	temperature coefficient for the PV module (1/K)
β_{air}	volumetric expansion coefficient of air (ideal gas) (1/K)
Δp	pressure drop through the closed loop collector (Pa)
ε	effectiveness of the heat exchanger
ε_{ab}	emissivity of the absorber plate
ε_g	emissivity of the glass cover
ε_{PV}	emissivity of the PV module
η_{Eref}	maximum electrical efficiency at reference conditions when the PV cell is at temperature T_{PVref} (%)
η_{el}	actual electrical efficiency of the PV system (%)
η_P	pump efficiency (%)
μ_w	dynamic viscosity of water (kg/m s)
ν_{air}	kinematic viscosity of air (m^3/s)
ρ_d	diffuse reflectance of the cover plate
ρ_w	density of water (kg/m^3)
σ	Stefan–Boltzmann constant (=5.67 × 10^{-8} W/m^2 K^4)
τ_{ab}	transmittance of the absorber plate
τ_g	transmittance of the cover plate (glass)
τ_{PV}	transmittance of the PV module
$(\tau\alpha)_{PV}$	transmittance–absorptance product for the PV module
$(\tau\alpha)_{ab}$	transmittance–absorptance product for the absorber plate

In residential buildings, where our study is based, solar systems can provide not only electricity, but also hot water and space heating (and/or cooling) depending on the specific end-user requirements, and of course the technology used. In particular, solar thermal collectors and photovoltaic (PV) systems are potential on-site renewable energy options; the former can provide heat for domestic hot water (and also possibly space heating, although this is not considered in the present study), while the latter can provide electricity to cover part of the household needs in electrical power. Therefore, there is a significant interest in the development and wider deployment of such systems, since these can form a basis for the achievement of the aforementioned energy targets, while decreasing the fossil-fuel based energy consumption in buildings [3]. However, further performance improvements, as well as investment in existing and future solar technologies are necessary in order to ensure the appropriate infrastructure, and to reduce the associated costs of these systems thus making them economically viable [4,5].

The present paper focuses on the holistic, distributed supply of both domestic hot water and electrical power to a representative household through a hybrid solar system. This concept has a very significant potential to achieve this goal, which arises from the synergistic combination within a single arrangement of a PV module and a solar thermal collector sub-system. This combination allows electricity and hot water to be generated simultaneously, while reducing the efficiency deterioration experienced by the PV module at elevated temperatures by cooling the PV module with a flow of water that is then used for the provision of hot water. The quantities of hot water and electricity used in households are strongly dependent on user behaviour. Therefore, in order to properly size and design a representative hybrid solar system for domestic heating and power, it is very important to define and to characterise these profiles [6].

The overall aim of this paper is to assess the annualised performance of a hybrid PV and solar thermal (PVT) system installed on the roof of an average three-bedroom terraced house located in

London, UK. The interest here is in investigating of the role of important system parameters in maximising the supply potential of both electricity and hot water in this particular scenario. An additional motivating factor is to maintain simplicity of design, leading to a minimisation of systems costs to the end-user. For this reason a commercially available PVT unit is chosen, and the unit's operational performance within an overall system for the provision of hot water and electricity generation are simulated over the course of a full year. This design is compared to a reference case based on the same house using conventional technologies, consisting of a combination of natural gas boilers, heat pumps and electrical heaters for hot water, and electricity bought from the grid.

In Section 2 we proceed to discuss the concept of a hybrid PVT system, review the literature and previous work in this area, and present a number of currently available commercial systems, along with a summary of their performance and cost. In Sections 3 and 4 we present the modelling methodology employed in our study, and discuss how the various system parameters where obtained or estimated. Also presented are details of the parametric analysis undertaken to evaluate the performance of our chosen PVT system for different design parameters; the aim of this analysis being to find the parameters which optimise the PVT system for our scenario of interest, i.e. the supply of domestic electricity and hot water to an average household in London. Following this, Section 5 contains the main results from the present study, together with a relevant discussion and, finally, the main conclusions from this work are stated in Section 6.

2. Hybrid PVT systems

2.1. Combined solar heat and power

Most of the solar radiation absorbed by a PV cell is converted to heat, increasing the temperature of the cell and decreasing its electrical efficiency [7–10]. To overcome this problem, solar cells can be cooled by a flow of a suitable fluid (gas or liquid), decreasing their temperature and improving their efficiency, while producing a useful thermal output. The synergistic combination of the improved electrical output and the associated heat-provision potential (for hot water provision and/or space heating) have motivated the development of *hybrid* PV/thermal (PVT) concepts [7–10], which have emerged as holistic solar energy solutions that combine a PV module for electricity generation, coupled with a heat exchanger arrangement and a coolant circuit containing a heat transfer fluid for heat provision from the same collector area [8,11–14].

The total energy output (electrical plus heat) of a hybrid PVT system depends on several factors, such as: the configuration design and heat extraction arrangement employed; the solar irradiance, ambient temperature and wind speed; and the operating temperatures of a number of important components. In most applications the electrical output is typically the main priority, in which case the operating condition of the heat transfer arrangement is adjusted to optimise electrical performance. Specifically, the cooling fluid (typically air or water) in the heat transfer circuit is kept at a low temperature in order to avoid an otherwise undesirable decrease in the electrical efficiency of the PV cell [8,10–12]. This constraint for the heat transfer fluid to exit the collector at low temperatures in order to allow higher electrical outputs imposes a limit on its posterior use for heating purposes. On the contrary, if the system were designed to provide higher fluid temperatures at the PVT unit outlet for use in applications such as water heating, then the electrical efficiency would decrease [8,10,12,15]. Hence, a design conflict arises between the electrical and thermal performance of hybrid PVT systems, and a trade-off is needed depending on the end-user needs and the local solar and environmental conditions. This conflict along with the elevated costs of PVT, are the two main reasons why these systems are currently not as widely employed as separate, individual PV and solar thermal collector equivalents [10].

2.2. Commercial systems and system selection

Although hybrid systems are not yet a fully mature technology and their commercialisation is still in its early stages, a small number of manufacturers are nowadays producing PVT air (PVT/a) and PVT water (PVT/w) systems, as well as concentrating systems. The performance of a variety of commercially available systems, in terms of both thermal and electrical output, along with the corresponding manufacturers is shown in Fig. 1.

This paper focuses on PVT/w systems, which feature a PV module placed in thermal contact with a water-based solar thermal collector. PVT/w systems are considered the most efficient way of preheating water over the course of a whole year [7,8,10]. Most of the PVT/w systems in Fig. 1 (red squares) are based by thermally attaching mono-crystalline PV modules on top of flat plate solar collectors [16–19]. It is important to note that most manufacturers of PVT/w systems have developed their systems by modifying commercially available solar collectors to include the PV module on its absorber surface [14]. The utilisation of the surface area that is exposed to the solar radiation is of primary importance and interest. When the PV cell is placed above the thermal collector section, in order to achieve high electrical performance, the presence of the PV leads to a reduction of the heat flux into the collector fluid circuit, reducing the module's thermal efficiency. Previous studies (e.g. [20,21]) investigated the trade-off between larger coverage areas for increased electricity generation and smaller coverage areas when the priority is hot water production, yet this trade-off is sensitive to the solar and environmental conditions at the geographical location of installation.

Of the different types of PVT/w system, configurations incorporating sheet-and-tube collectors are considered particularly promising options for domestic hot water production [22]. Even though they perform marginally worse than channel collectors (typically by ~2%; [22]), they are a good option in terms of thermal efficiency (58%; [22]) and, importantly, are a simple and low-cost configuration to manufacture, as they only require the integration of a standard PV panel with a standard thermal collector with no major modifications, relying on mature and widely available technologies. In addition, the results in Ref. [22] indicate that although a sheet-and-tube collector with two covers has a slightly higher

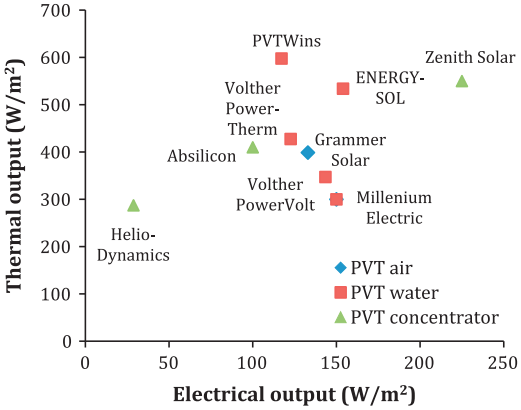

Fig. 1. Summary of commercially available hybrid PVT systems: PVT/a (blue diamonds), PVT/w (red squares) and concentrated PVT (green triangles), all in terms of their thermal vs. electrical output (W/m^2). (For interpretation of the references to colour in this figure legend, the reader is referred to the web version of this article.)

thermal efficiency at elevated water temperatures compared to a single-cover collector, its electrical efficiency deteriorates considerably due to the second cover. Thus, we consider the single-cover sheet-and-tube PTV/w collector as a highly suitable starting point towards the achievement of a favourable trade-off between thermal and electrical output, at a reasonable cost.

Numerous studies [10,12,13,16,17,23] have compared the electrical and thermal performance of PVT systems to that of separate PV modules and solar thermal collectors. An important finding is, once again, that beyond the choice of the configuration, the performance of these systems is highly dependent and geographical location [23]. Tripanagnostopoulos et al. [8] found that PVT/w systems have slightly higher electrical efficiencies compared to standard PV modules, however, other studies concluded that the electrical output of PVT systems is actually lower (e.g. by ~38% in Ref. [11]) because of the higher operating temperatures and the additional glazing. Further, PVT collectors can be less efficient than conventional solar thermal collectors in extracting heat, due to the reduced conductivity of the absorber and limitations imposed by the presence of the PV module. The studies of Tripanagnostopoulos [10] and Vokas et al. [23] are in agreement with respect to this point, that latter showing a lower value (of around 9%) for the thermal efficiency of a PVT system compared to conventional solar thermal collectors. Another study undertaken in Taiwan (see Ref. [15]) reported that the thermal and electrical efficiencies of a hybrid PVT/w system was better than the efficiencies of separate, conventional solar water-heating collectors and PV modules, with a thermal efficiency of up to 38%, a primary-energy saving efficiency of more than 60% and a PV efficiency of 9%.

In any case, a distinctive characteristic of PVT collectors is the dual output of electricity and hot water, so that even in the case that both the yields are slightly lower in a PVT system than in conventional PV and solar thermal systems (as in, e.g. Ref. [14]), the PVT system generates both heat and electricity from the same surface area, as opposed to separate, individual side-by-side PV panels and solar thermal collectors [22,24]. Hence, an additional advantage appears when the available external building surface is limited, above and beyond the fact that PVT systems constitute an integral unit, which is considered more aesthetically pleasing, providing greater architectural uniformity than separate systems with a different appearance [10,13,22].

Another aspect of hybrid technologies that is of particular interest concerns the circulation of the cooling fluid. Thermosyphon systems have been identified as a good option in warm locations with subtropical or temperate climate conditions [9,25]. However, at higher latitudes (i.e. colder regions such as the UK, which is of direct interest to the present study) the outdoor temperatures can remain below the freezing point of water, typically for more than a third of the year, in which case the addition of antifreeze liquid into the fluid circuit reduces their thermal performance by about 15% [11,26], and makes them a less appropriate solution.

In conclusion, the extent and specific area layout/coverage of hybrid PVT systems, as well as the mode of the fluid circulation, appear as two specific system parameters of particular interest, as is the specific evaluation of the performance of hybrid PVT system in a particular climate, which in this work is the UK. Fig. 1 indicates that amongst the commercially available PVT systems, an excellent option in terms of combined thermal *and* electrical output is the concentrating PVT system of Zenith Solar but this unit is not suitable for roof-top domestic installation as it requires solar tracking. Therefore, two very appropriate options amongst the available PVT/w systems are the systems manufactured by PVTWins [18] and by ENERGIES-SOL [16]. In the present paper we have selected the latter for further analysis and examination, as it provides the highest electrical output while maintain a similar thermal output per unit surface area.

3. Modelling methodology

The core components of the complete hybrid PVT/w system that we will focus on in this paper are: (i) the PVT collector; (ii) a hot water (thermal) storage tank; (iii) an auxiliary heater necessary to meet the temperature requirements of the end-user when the solar supply is insufficient; (iv) a water circulator pump; and (v) interconnecting pipework [7,14]. In our approach, we have split the overall system into two separate sub-systems: (i) the PVT unit with its active, closed water loop, including the pump (Section 3.1); and (ii) the hot water storage tank and the auxiliary heater (Section 3.2). The two sub-systems interface at the storage tank, where they are connected by a heat exchanger located inside the tank. In this heat exchanger heat is transferred from the water circuit flowing through the solar collector to the water in the tank.

3.1. PVT/w unit modelling

3.1.1. PVT/w unit description

The two main components of the PVT/w unit are the PV module and the rest of the solar collector, which can be further divided into the glazing, the thermal absorber, the riser water tubes and the insulation layer. Similarly to previous PVT modelling attempts [3,22,27,28], energy balance equations were written in order to calculate the heat transfer rates and temperatures throughout the unit. The equations were applied separately to each layer of the PVT unit, instead of using global equations to find the average absorber plate temperature and the energy flows [24,29]. This allowed an estimation of the average temperatures of all the separate unit layers with the aim of defining the system state more accurately. Based on the large Fourier numbers (characterising the ratio of thermal conduction to unsteadiness) of our problem, a quasi-steady assumption was made, according to which the panel was assumed to be in thermal steady-state at each time instant.

In more detail, the PVT unit modelled in this paper is based on the commercially available hybrid system ENERGIES-SOL, as presented in Ref. [16]. In addition, a few typical parameters were needed from the literature [3,22,24,30,31], in order to fully define the system. The ENERGIES-SOL unit consists mainly of (from top to bottom): a transparent cover (glass), an air gap, a mono-crystalline (c-Si) PV module, an EVA encapsulating film, an absorber–exchanger which transforms the solar radiation to heat and transfers it to the collector fluid, and a layer of insulation material at the bottom (Fig. 2). The backside/underside, and also side insulation (not shown here) layers reduce heat losses, while improving structural strength. The absorber–exchanger consists of a sheet-and-tube heat exchanger in which water flows in parallel pipes (eleven copper riser tubes) from the header inlet pipe to an outlet pipe on the upper side of the collector that collects the warm fluid [32]. The transparent cover is a single glass sheet with a thickness of 3.2 mm [16,22,24].

Although the commercially available ENERGIES-SOL PVT collector unit is completely covered by PV modules over its entire surface area, our model of this unit splits the collector into two sections (Fig. 3): (i) a PV-covered section that occupies a (variable) fraction P of the total collector area; and (ii) an uncovered section that occupies the remainder of the area. This was done in order to study the effect of coverage of the unit with PV, by allowing a direct adjustment of the relative importance of the unit's electrical and thermal outputs.

As shown in Fig. 3, the overall PVT arrangement comprises an active closed-loop system in which, in normal operation, the collector

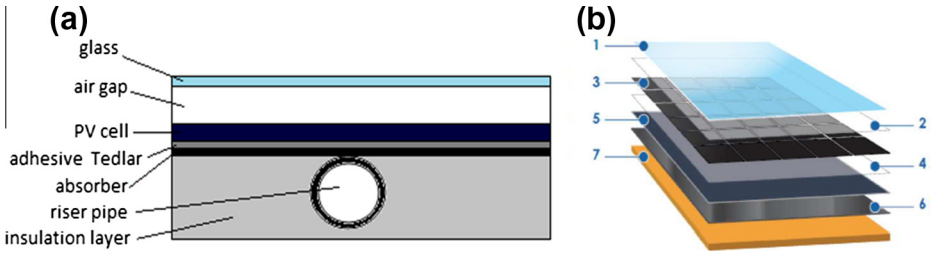

Fig. 2. Referring to the PV-covered section of the PVT collector (#2 in Fig. 3): (a) PVT collector cross-section. (b) PVT layers: 1. Tempered glass (high transmittance), 2. EVA encapsulating film, 3. c-Si PV cells, 4. EVA encapsulating film, 5. Adhesive plus back-sheet Tedlar, 6. Aluminium absorber plate plus solar collector, 7. Insulating layer. Taken from Ref. [25]. The uncovered collector section is identical, but without the PV, EVA, adhesive and Tedlar layers (3–5).

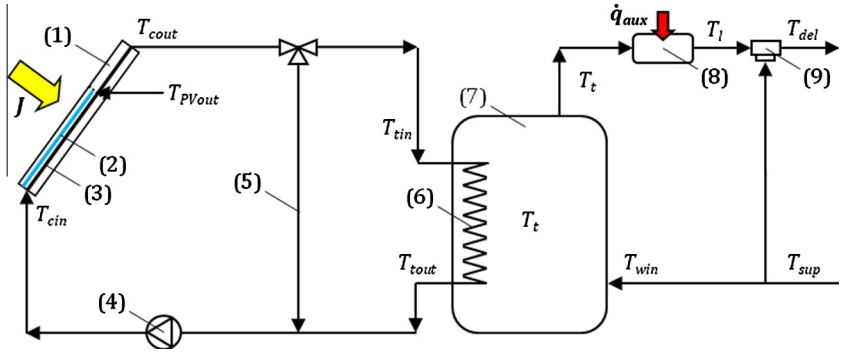

Fig. 3. Schematic diagram of the full PVT domestic hot water system: 1. Solar collector/PVT unit, 2. Section (area fraction $P = A_{PV}/A_c$) of the collector covered by PV, 3. Cooling water flow tubes, 4. Water pump (flow-rate $\dot{m}_c$, V_P), 5. By-pass, 6. Tank heat exchanger, 7. Water storage tank, 8. Auxiliary heater, 9. Mixing device for final temperature delivery regulation.

outlet flow (flow-rate $\dot{m}_c$ and temperature T_{cout}) enters the heat exchanger located inside the hot water storage tank (flow-rate $\dot{m}_t = \dot{m}_c$ and temperature $T_{tin} = T_{cout}$), heats the water in the tank (mass M_t and temperature T_t), exits the tank (temperature T_{tout}) and returns to the inlet of the solar collector (temperature $T_{cin} = T_{tout}$) to be heated again. A bypass valve is required to control the temperature of the water leaving the collector and entering the tank ($T_{tin} = T_{cout}$), and to ensure that this stream only heats (and does not cool) the water in the hot water storage tank. This bypass is controlled by a differential on/off solenoid valve that sends the collector fluid flow to the tank only when the outlet flow temperature from the collector is greater than the temperature of the water in the storage tank, or $T_{cout} > T_t$. If this is not the case, the fluid is returned to the collector via the bypass connection for further heating, such that $T_{cin} = T_{cout}$ [32].

The PVT/w model developed in the present work has been developed under the following assumptions:

- The fraction of solar irradiance that is not converted into electricity in the PV cells and is not lost to the environment is transmitted to and absorbed by the absorber plate in the form of heat [31].
- The PV cells and the absorber plate are in perfect thermal contact [31].
- Heat transfer (losses) at the sides of the PVT collector are negligible [28].
- The heat capacities of the PVT system components (PV cells, Tedlar and insulation) are negligible compared to the heat capacity of water [30].
- The optical properties of the glass cover, absorber plate and PV cells are constant; for simplicity, the transmittance of the EVA layer is assumed to be unity [30].
- The water flows through the PVT collector tubes are uniform, with the total mass flow-rate divided equally among all (eleven) tubes running through the collector [3].
- The pipes connecting the PVT unit with the water storage tank are well insulated, such that there are no heat losses to the environment [31].
- The system is in steady state [22,30], based on the justification made early in this section.

3.1.2. PVT unit model equations

In each section (PV-covered and uncovered) and for each layer in that section (see Figs. 2 and 3), an energy balance considering radiative, convective and conductive thermal exchanges between the layers, the cooling water flow and the environment (where relevant) is applied. A spatially averaged temperature is taken across the different sections of each layer [30]. The equations that result from these balances, and which are detailed in the proceeding sections below, are solved at 48 half-hourly time steps ($i = 1$–48) in order to estimate the performance of the system throughout a day.

3.1.2.1. PV-covered section. After neglecting the absorption of solar radiation by the front/top layer (glass cover), given the very low absorptivity of glass ($\alpha_g = 0.05$), the energy balance for the glass cover is (using heat fluxes, i.e. per unit area),

$$\dot{q}_{sky}A_{PV} + \dot{q}_{wind}A_{PV} = \dot{q}_{rPV}A_{PV} + \dot{q}_{ag}A_{PV}. \quad (1)$$

The first heat flux term on the LHS of Eq. (1) is given by [33,34],

$$\dot{q}_{sky} = \varepsilon_g\sigma\left(T_g^4 - T_{sky}^4\right), \quad (2)$$

with $T_{sky} = 0.0552T_a^{1.5}$ [28,33], while the second term is given by,

$$\dot{q}_{wind} = h_{wind}(T_g - T_a). \quad (3)$$

Various expressions are given in different sources for the estimation of h_{wind} [3,28,33,35]. These expressions do not differ significantly, and so it was decided to use the expression that provides intermediate values, within the range of the various predictions, which is $h_{wind} = 4.5 + 2.9v_{wind}$, and v_{wind} is taken here as 5 m/s

[36]. Since the wind speed is not constant, an average between the forced convection coefficient from Eq. (3a) and a free convection coefficient (without wind) is considered.

A radiative heat balance between two infinite parallel plates can be applied to the first RHS term in Eq. (1), which describes the heat transfer from the glass cover to the PV laminate (adapted from Ref. [33]), such that,

$$\dot{q}_{rPV} = \frac{\sigma(T_{PV}^4 - T_g^4)}{1/\varepsilon_{PV} + 1/\varepsilon_g - 1}. \quad (4)$$

Finally, heat can be transferred from the glass cover through the air gap to the PV laminate by convection, conduction, or both. The convective heat transfer coefficient can be estimated from knowledge of the Nusselt number ($Nu = h_w D/k_w$), which can be related by means of correlations to the Grashof number ($Gr = g\beta_{air}\Delta T L^3/\nu_{air}^2$) [33]. A 5 mm plate spacing (gap size) leads to a value for Gr ($\approx$68) that is 4 orders of magnitude lower than that required in common correlations for Nu (i.e. 10^4–10^7). Thus, natural convection within the air gap is neglected and, consequently, it is assumed that heat transfer through the air gap is mainly due to conduction,

$$\dot{q}_{ag} = \frac{k_{air}}{e_{ag}}(T_{PV} - T_g). \quad (5)$$

Having considered the glass cover (first layer), the energy balance for the PV laminate below is,

$$(\tau\alpha)_{PV} J A_{PV}(1 - \eta_{el}) = A_{PV}(\dot{q}_{rPV} + \dot{q}_{ag} + \dot{q}_{ca}). \quad (6)$$

Following Ref. [33] the transmittance–absorptance product is calculated from $(\tau\alpha)_{PV} = \frac{\tau_g \alpha_{PV}}{1-(1-\alpha_{PV})\rho_d}$ with $\rho_d = 0.16$, while J is the incident global solar irradiance *on the tilted PVT collector surface*, which has been placed at the optimal inclination angle and orientation that maximises the annual solar irradiation in London, UK (see Section 4.2). The PV efficiency depends on the module temperature and is estimated from the expression $\eta_{el} = \eta_{Eref}[1 - \beta_0(T_{PV} - T_{PVref})]$ [37], where $T_{PVref} = 25$ °C at an irradiance of 1000 W/m^2 (manufacturer-stated values) and β_0 is also given in the technical specifications of the ENERGIES-SOL system being considered here.

Furthermore, the heat flux from the PV module to the absorber plate on the RHS of Eq. (6) can be found from,

$$\dot{q}_{ca} = G_{ca}(T_{PV} - T_{ab}). \quad (7)$$

The PV laminate is composed of the following layers: a c-Si wafer, which has a very high thermal conductivity compared with the other layers (with $k \approx 149$ W/m K) and is therefore neglected; a 50 μm thick layer of highly conductive glue that minimises thermal resistance ($k = 0.85$ W/m K); a 0.1 mm thick PE-Al-Tedlar layer ($k = 0.2$ W/m K); and a 0.5 mm EVA layer ($k = 0.35$ W/m K) [16]. Based on these thicknesses and thermal conductivities, the heat conductance (inverse of resistance) of the entire PV laminate layer as this appears in Eq. (7) is determined as $G_{ca} = (R_{EVA} + R_{ted} + R_{glue})^{-1} = (\frac{5\cdot10^{-4}}{0.35} + \frac{1\cdot10^{-4}}{0.20} + \frac{5\cdot10^{-5}}{0.85})^{-1} = 500$ W/m^2 K.

In addition, the heat flux term $\dot{q}_{ca}$ in Eqs. (6) and (7) is related to the heat transferred from the absorber layer to the water flow plus that lost through the backside/underside insulation layer to the environment, or,

$$\dot{q}_{ca} = \dot{q}_{bi} + \dot{q}_w, \quad (8)$$

where the heat flux lost to the environment through the backside layer insulation is,

$$\dot{q}_{bi} = G_{bi}(T_{ab} - T_a). \quad (9)$$

The heat transfer conductance between the absorber and the environment (through the backside layer insulation) that appears in Eq. (9) is calculated from $G_{bi} = (R_i + R_{air})^{-1} = (\frac{e_i}{k_i} + \frac{1}{h_{airi}})^{-1}$, where h_{air} is the free convective heat transfer coefficient of air at the underside of the PVT module assuming that the effect of the wind is negligible, such that this can be calculated from Eq. (3) with $v_{wind} = 0$ m/s.

Similarly, the convective heat transfer from the absorber layer to the cooling water flow can be related to the temperature difference between the absorber plate and the (bulk) water stream,

$$\dot{q}_w = h_w(T_{ab} - T_{bw}). \quad (10)$$

Here, the bulk water stream temperature T_{bw} is estimated as an average temperature between the water entering the collector T_{cin} and the water exiting the PV covered part T_{PVout} (refer to Fig. 3), i.e. $T_{bw} = (T_{PVout} + T_{cin})/2$, and the heat transfer (flux) from the absorber to the water can be estimated from,

$$\dot{q}_w = \dot{m}_c c_p (T_{PVout} - T_{cin}). \quad (11)$$

In order to evaluate the convective heat transfer coefficient of the water flow in the pipes h_w that appears in Eq. (10), the nature of the flow condition must be established. This is done by considering the Reynolds number ($\mathrm{Re} = \rho v D/\mu_w = 4\dot{m}_{tube}/\pi D\mu_w$). In the present investigation we have confirmed that the condition $Re < 3000$ is always met, such that the flow is always laminar. For laminar flow, and assuming fully developed conditions, the appropriate heat transfer coefficient correlation is used, which is $Nu = h_w D/k_w = 4.36$ [34].

Finally, the PVT unit electrical power output is calculated from the irradiance normal to the collector plane J,

$$P_{PV} = J A_{PV} \eta_{el}, \quad (12)$$

and the *net* power output P_{net} accounts also for the power consumed by the water pump P_P and the electrical demand at that time of the day, P_{wd} or P_{we}, depending on whether it is a weekday or a weekend day, such that,

$$P_{net} = P_{PV} - P_P - \{P_{wd}; P_{we}\}. \quad (13)$$

3.1.2.2. Uncovered collector-only section. The energy balance for the front/top layer (glass cover) of the solar collector section that is not covered by PV is very similar to the PV-covered equivalent stated above, but in this case applied to the area $A_c\,(1 - P)$,

$$A_c(1 - P)(\dot{q}_{skya} + \dot{q}_{winda}) = A_c(1 - P)(\dot{q}_{rab} + \dot{q}_{agab}), \quad (14)$$

where $P = A_{PV}/A_c$, and the heat flux terms $\dot{q}_{skya}$, $\dot{q}_{winda}$, $\dot{q}_{rab}$ and $\dot{q}_{agab}$ are calculated using the same method as for the covered section, i.e. Eqs. (2)–(5), with the absorber layer replacing the PV layer.

Proceeding to the next layer in this section, the energy balance for the absorber plate is,

$$(\tau\alpha)_{ab} J A_c(1 - P) = A_c(1 - P)(\dot{q}_{rab} + \dot{q}_{agab} + \dot{q}_{caab}), \quad (15)$$

where $(\tau\alpha)_{ab}$ is calculated from the expression provided below Eq. (6) with the absorber replacing the PV, i.e. $(\tau\alpha)_{ab} = \frac{\tau_g \alpha_{ab}}{1-(1-\alpha_{ab})\rho_d}$, and $\dot{q}_{caab}$ is calculated similarly to Eq. (9) with G_{ca} assumed equal to that in the covered section since the only difference is the thermal conductivity of the c-Si layer that is considered negligible.

Similarly, this heat $\dot{q}_{caab}$ can be transferred to the water $\dot{q}_{wab}$ or lost through the insulation layer $\dot{q}_{biab}$,

$$\dot{q}_{caab} = \dot{q}_{biab} + \dot{q}_{wab}, \quad (16)$$

where $\dot{q}_{wab}$ and $\dot{q}_{biab}$ are again calculated using the same methods as in the covered section, Eqs. (9)–(11).

3.1.2.3. Power and pressure drop. The household electrical demand (see Section 4.1 for details) is imposed as an input to the model and the power consumed by the water pump of the PVT system is calculated from,

$$P_P = \frac{\Delta p Q}{\eta_p}, \quad (17)$$

where η_P is taken as constant and equal to 0.85 [38], and Δp can be evaluated as the superposition of major losses caused by friction and minor losses in the bends and fittings due to the flow of water,

$$\Delta p = f\frac{L}{D}\left(\frac{1}{2}\rho_w v_w^2\right) + \sum K_S\left(\frac{1}{2}\rho_w v_w^2\right). \quad (18)$$

In this work the flow is laminar in all conditions (justification given below Eq. (11)), such that $f = 64/Re$.

3.2. Water storage tank modelling

On the other side of the system from the PVT unit (refer to Fig. 3), cold water from the mains (temperature T_{sup}) flows into the tank (temperature $T_{win} = T_{sup}$) where it is mixed with the water already contained therein to a temperature T_t. When there is a demand from the household for hot water, water (temperature T_t) is drawn from the tank. An auxiliary heater is placed at the outlet of the hot water tank, which is necessary in order to meet the temperature requirements of the end-user when the solar supply is insufficient. Finally, in the case that hot water is required at a temperature lower than the tank water temperature ($T_{del} < T_t$), a mixer is introduced to cool the water from the tank before it is directed to the house. The mixer is not considered in our model since, in the interests of studying the most demanding scenario and for simplicity of design, a constant hot water supply temperature catering to a constant demand temperature of $T_l = T_{del} = 60$ °C is used.

In addition to the assumptions listed previously, the following assumptions are applied to the tank model:

- The tank only loses heat [31], e.g. it does not gain solar heat.
- The storage tank is fully mixed, that is, there is no stratification due to the forced mode of operation and continuous supply of hot water load [3,30,39].

An energy balance on the tank can be discretised in time and solved at 30-min intervals, such that the water temperature in the tank at each time-step $T_t\,(i+1)$ is calculated from the various heat fluxes at the previous time-step [39], that is,

$$M_t c_p \frac{T_t(i+1) - T_t(i)}{\Delta t} = \dot{q}_{ct}(i) - \dot{q}_{loss}(i) - \dot{q}_{load}(i). \quad (19)$$

In Eq. (19), the heat losses through the walls at time-step i can be evaluated by,

$$\dot{q}_{loss}(i) = S_t U_t [T_t(i) - T_{as}], \quad (20)$$

and the energy removal to supply the domestic hot water demand is,

$$\dot{q}_{load}(i) = \dot{m}_l(i) c_p [T_t(i) - T_{win}], \quad (21)$$

where water enters the tank is at the mains supply temperature $T_{win} = T_{sup} = 10 \pm 2.6$ °C in the UK [40].

To evaluate the rate of thermal energy transfer from the collector to the water storage tank at time (i), the bypass setting (#5 in Fig. 3) must be accounted for, since heat is only added to the tank when the temperature of the water exiting the collector is higher than the temperature of water in the tank, $T_{cout}(i) > T_t(i)$. Otherwise, there is no heat addition, that is, $\dot{q}_{ct}(i) = 0$. The heat added to the tank $\dot{q}_{ct}(i)$ is evaluated by considering the heat transfer across the heat exchanger located inside the tank. According to Ref. [35], the most practical approach towards heat exchanger design for solar systems is based on the *NTU*-effectiveness (ε) method. Thus, the rate of energy added from the collector to the tank, $\dot{q}_{ct}(i)$, is calculated from,

$$\dot{q}_{ct}(i) = \varepsilon \dot{m}_c c_p [T_{cout}(i) - T_t(i)], \quad (22)$$

and the temperature at the outlet of the heat exchanger immersed in the tank, T_{tout}, is,

$$T_{tout}(i) = T_{cout}(i) - \varepsilon [T_{cout}(i) - T_t(i)]. \quad (23)$$

As this system is a closed loop, this will also be the temperature entering the collector at next time-step,

$$T_{cin}(i+1) = T_{tout}(i). \quad (24)$$

The effectiveness ε can be predicted directly from the characteristics of the heat exchanger and the relevant flows. The equations to determine this parameter can be simplified in situations where the temperature on one side of the heat exchanger are constant, as with a coil in a (non-stratified, uniform) tank, as is assumed to be the case in the present study. Then, the effectiveness ε and *NTU* are calculated from:

$$\varepsilon = 1 - e^{-NTU}; NTU = \frac{(UA)_t}{(\dot{m}c_p)_s} = \ln\frac{1}{1-\varepsilon}. \quad (25)$$

The overall heat transfer coefficient in the tank heat exchanger, ignoring conduction through the walls, is,

$$\frac{1}{(UA)_t} = \frac{1}{h_i A_i} + \frac{1}{h_e A_e}, \quad (26)$$

where the subscripts i and e refer to the fluid flow inside and the fluid outside the coil, respectively. In the particular case of a coil immersed in a water tank, it is expected that $h_i \gg h_e$ due to the (enhanced) forced convection experienced as a result of the higher flow speeds inside the coil, while the water in the tank experiences only free convection. Therefore, the limiting resistance is that due to free convection in the tank. The correlation used to calculate this coefficient for immersed (external flow) geometries is [34],

$$Nu = \frac{hL}{k} = CRa^n, \quad (27)$$

where $C = 0.52$, the Rayleigh number ($Ra = Gr{\cdot}Pr = g\beta(T_s - T_\infty)L^3/\nu\alpha$) is based on a characteristic length L of the geometry (in this case the tube diameter D), and the exponent $n = 1/4$ for laminar flow.

Finally, as stated previously, an auxiliary heater is used in order to cover the hot water demand requirements when the storage tank temperature T_t (here in °C) is lower than 60 °C. The additional heat necessary is,

$$\dot{q}_{aux}(i) = \dot{m}_l(i) c_p [60 - T_t(i)]. \quad (28)$$

3.3. Annual performance calculations

The model developed to assess the PVT system performance provides results on a diurnal basis. These results are then used to calculate the monthly outputs of the system for the different months of the year, with the final aim of obtaining total annual outputs. The input data to the model are average daily profiles of: solar irradiance, ambient temperature, hot water demand and electricity demand, all over a 24-h period. These inputs vary depending on the month of the year, and the electricity demand also depends on whether it is a weekday or weekend day. Hence, the PVT system model is run 24 times (12 months; one average weekday and one average weekend day per month), and the outputs are compiled and suitably weighted for weekdays and weekends to obtain total monthly and annual performance results [41]. Each daily run comprises 30-min intervals, such that the 24-h period is divided into a set of 48 time steps, assuming that all parameters and variables are constant during each time interval. Then, for example, for the total yearly electricity demand,

$$E_T = \sum_{1}^{12}\left\{\frac{261}{12}\sum_{i=1}^{48}E_{wd}(i) + \frac{104}{12}\sum_{i=1}^{48}E_{we}(i)\right\}, \quad (29)$$

where $E_{wd}(i)$ and $E_{we}(i)$ are the average household electricity demands on a weekday and a weekend day respectively, and i represents each half-hour interval for which the model was run. This equation is applied similarly to each output or other variable of interest from the PVT system model to obtain total annual results, which are then used for the comparison of the performance of different system configurations.

Two important PVT system performance indicators are the percentages of the household electricity and hot water demands covered by the PVT system outputs. The total annual values of these key performance indicators are calculated from the results of equations such as Eq. (29), as follows:

$$DC_E(\%) = \frac{E_{PVT} - E_{loss}}{E_T}\cdot 100; DC_{HW}(\%) = \frac{Q_{PVT}}{Q_T}\cdot 100, \quad (30)$$

where E_{PVT} and Q_{PVT} are the *raw* electrical and *net* thermal energy (for hot water production) outputs of the PVT system, and E_{loss} are the electrical pumping losses, all over a full year. In addition, E_T and Q_T are the total annual electricity and hot water household demands, respectively. Note that E_{PVT} is related to the (typically −ve) *net* electrical energy available *from* the PVT-supported household E_{PVTnet}, via $E_{PVTnet} = E_{PVT} - E_{loss} - E_T$.

In order to compare the integrated (electricity plus heat) performance of the different configurations studied, two additional parameters are considered. These are the average percentage of demand covered (DC_{av}) and the weighted average percentage of demand covered by the PVT system throughout the year (DC_{wav}):

$$DC_{av}(\%) = \frac{DC_E + DC_{HW}}{2}; DC_{wav}(\%) = \frac{E_T DC_E + Q_T DC_{HW}}{E_T + Q_T}, \quad (31)$$

which are average measures of the *combined* electrical and thermal household demands covered by the PVT. The former is a direct arithmetic mean of the two covered demands, while the latter is a weighted mean that takes into account the contribution of the actual amounts of electrical and thermal energy demands.

3.4. Environmental assessment

Beyond studying the performance of the modelled PVT unit, a further goal of this work is to estimate the possible emissions savings made by the installation of such a system compared to the emissions associated with the use of *conventional* means, based on the common current practices of buying the electricity from the grid, and using a boiler, heat pump or electrical heater to satisfy the hot water demand (see Section 4.3).

With regards to electricity, the emission saving is due to the difference between the emissions associated with the purchase of all electricity from the grid (Em_{cE}) and the emissions incurred after a PVT unit is installed (Em_{PVTE}), while the hot water saving arises from the reduction in the required primary fuel for heating, from the conventional levels (Em_{cHM}) to the lower auxiliary heating levels needed by the PVT system (Em_{aux}),

$$Em_{sE}(\%) = \frac{Em_{cE} - Em_{PVTE}}{Em_{cE}}\cdot 100;$$
$$Em_{sHW}(\%) = \frac{Em_{cHW} - Em_{aux}}{Em_{cHW}}\cdot 100. \quad (32)$$

The hot water emission terms are calculated, by considering a typical/average UK household heating mode that features a mix of gas boilers, heat pumps, etc., representative of the UK. This is discussed in Section 4.3.

4. Model parameters

4.1. Reference house

A reference house is required for the estimation of the hot water and electricity consumptions, as well as the available roof for the installation of the system. According to Ref. [42], the most common type of house in London is a terraced house, with an average number of about 3 bedrooms. An average number of 4 inhabitants is assumed; 2 adults and 2 children. A floor area of around 70–90 m^2 is expected in this house [43]. The average available roof area for the installation of solar systems is 15 m^2 [44].

4.1.1. Electricity demand profile

The electricity demand profile of an individual dwelling is more difficult to define as it depends strongly on the activities of the occupants as well as the electrical appliances available and their associated use [45]. A number of different models and profiles have been reviewed, with studies undertaken in Sweden [6,41] and also in the UK [45]. The UK study, which includes a model developed by the Centre for Renewable Energy Systems Technology (CREST), has been selected here for our calculations because it combines both the patterns of active occupancy (considering when inhabitants are at home and awake) and their daily activity profiles, covering all commonly used appliances in a domestic dwelling in the UK. Furthermore, the configuration of these appliances considers their mean total annual energy demand along with their associated power-use characteristics, such as their steady-state consumption or typical use cycles. The active occupancy reflects the natural behaviour of real people in their daily lives and it is represented as an integer that varies throughout the day in a pseudo-random way. In order to create the active occupancy profiles, data derived from the UK 2000 Time Use Survey (TUS) about how people spend their time in the UK is used. Finally, the share of appliances as well as their correlated use is considered. The temporal resolution is 1-min with a 365 day simulation, which yields 525600 data points [45].

This model [45] was validated against the electricity demand of 22 dwellings in the town of Loughborough in the East Midlands (UK), recorded over a 1-year period. It also takes into account lighting, by considering the level of natural daylight when calculating the electrical light needed [45]. As it is available online as an Excel file [46], it is possible to estimate the electricity demand profile for the reference house studied in the present work by introducing 3 inputs: the number of residents in the house, the month, and whether it is a weekday or a weekend. The appliances are then randomly allocated and the electricity demand is estimated. An example of the output provided by the simulation for a July weekday in a house with 4 occupants is shown in Fig. 4(a).

The average annual electricity consumption per dwelling over the whole set of synthetic data is 4124 kW h, which is close to the 4172 kW h mean demand from the measured data (for the 22 measured buildings) [45]. In the simulation carried out in the present work the annual consumption is taken as 4500 kW h, a value in accordance to the previous data obtained and also in the range of 4400–4500 kW h/year given in Ref. [41].

The profile shown in Fig. 4(a) is in agreement with a study undertaken in England of the domestic load of 8 homes, in which the typical demand had a base load of ~0.5 kW, with peaks in the morning and evening of up to 4 kW [47]. Although the 1-min resolution is more accurate in reflecting the actual consumption, data averaging was done to find mean load values in 30-min intervals in the interest of data management.

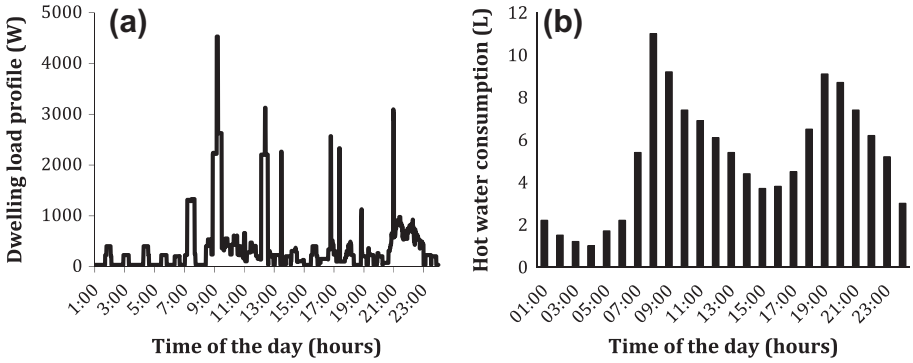

Fig. 4. (a) Electrical power load profile (1-min resolution) for a UK house of 4 inhabitants over a weekday in July [55]. (b) Diurnal hot water consumption profile used in this work, according to Ref. [53].

4.1.2. Hot water demand profile

The hot water demand varies considerably depending on the consumer and throughout the day/month/year, with a higher consumption but at a lower temperature requirement in the summer, and strong day-to-day variations. Nevertheless, it is possible for simplicity of analysis and greater transferability of the results to define and employ a repetitive average daily load profile and a daily averaged value for further investigations [13]. In particular, a study of domestic hot water consumption in 124 dwellings in England revealed that the mean household hot water consumption is 122 L/day, with a 95% confidence interval of ±18 L/day [48]. The same study demonstrated month-to-month consumption variations in the range −20 L/day (minimum, July) and +10 L/day (maximum, December), or between −16% and +8% respectively. Introducing these variations would not influence the results in the present modelling work, since the thermal energy output of the PVT system is found to be always lower than the instantaneous household demand by more than this amount (see Fig. 8(b)). Even so, a real system may experience significant instantaneous hot water-related performance variations due to a mismatch between the instantaneous supply and demand.

The study in Ref. [48] also found a hot water delivery temperature with a mean value of 51.9 °C ± 1.3 °C, although normally a boiler is expected to provide water at 60 °C [26,39]. In addition, the water mains temperature was reported as 10 ± 2.6 °C [40], so a value of 10 °C was used in the present work. A representative average daily profile is sought that can be repeated each day for simplicity [11,39]. Given the lack of a universal profile, it was deemed reasonable to employ the average profile of hot water consumption found in the study undertaken in the UK (in Fig. 4(b)) [48]. This is in line with related studies that use an approximate estimate of the daily consumption for a family of four of 120 L at 50 °C [13].

4.2. Solar irradiance availability

The Photovoltaic Geographical Information System (PVGIS) online tool is a map-based inventory of solar energy resources [49]. This database was used to obtain solar intensity profiles over the course of an average day in each month with a 15-min resolution, giving as outputs the global irradiance, J (W/m^2), on a fixed user-defined plane, along with the ambient temperature. Each value returned represents an average measurement over a 10-year period (1981–1990). A 36° (to the horizontal) inclination angle and South-facing orientation were selected, since they define an optimally tilted plane for maximum annual solar irradiation in London. Averages between two consecutive values were used to obtain the 30-min resolution input data required by our model. Fig. 5 shows the solar irradiance and ambient temperature for different months. Significant differences are observed between winter and spring/summer, with the latter having almost three times higher irradiance. This is expected to affect strongly the outputs of the PVT system during the different seasons.

4.3. Environmental assessment parameters

In order to undertake this assessment, the CO_2 equivalent emissions associated with grid electricity and natural gas burning are required, as applied to the UK. The values assigned to these parameters in this work were taken from Ref. [58]: 0.5246 kg CO_2(e)/kW$_e$ h for electricity and 0.1836 kg CO_2(e)/kW$_{th}$ h for natural gas.

The average annual end-user demands for hot water heating and electrical power (which are known, from Fig. 4) are different from the average annual household demands for natural gas (from the mains) and electrical power (from the grid). This is because

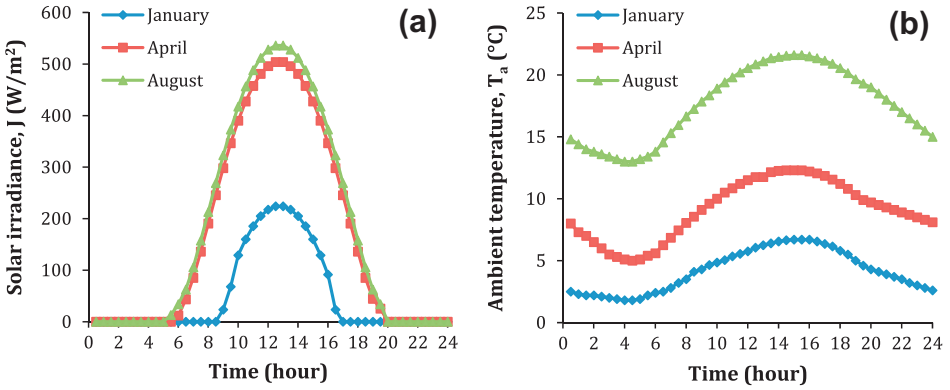

Fig. 5. (a) Diurnal solar irradiance and (b) average ambient temperature in January, April and August in London.

although all electrical demand is covered by the grid, the heating demand is, on average, satisfied not only (although mostly) by natural gas, but also to some extent by the grid (with electrical heaters and heat pumps). In this study the end-user heat and power demands have been converted to household gas and electrical demands by considering UK-specific data on the current uptake of boilers, air and ground source heat pumps, and electrical heaters and their respective efficiencies or Coefficients of Performance (COPs). Based on these data, the following expressions have been obtained:

$$Q_{gas} = \frac{0.97}{0.88} \cdot Q_{aux}; E_{grid} = \left(1 + \frac{0.03}{1.5} \cdot \frac{Q_{aux}}{E_{net}}\right) \cdot E_{net}, \quad (33)$$

where Q_{aux} and E_{net} represent the auxiliary heat and the electricity required to cover the demand, or in other words the short-fall between the demand and the amount produced by the PVT system. These expressions can also be used to calculate the CO_2 emissions incurred to cover these demands.

The following data were used to obtain these factors:

- About 3% of the total boilers in the UK are electrical heaters and heat pumps, with the two systems being employed equally (typically about 20000 new units per year in 2010). Air source heat pumps are more commonly used by about a factor of 3 times, relative to ground source equivalents [50].
- The average boiler efficiency is 88% [51]. This value is dominated by the vast majority of high-efficiency condensing boilers (98.9% of all newly installed boilers in the UK).
- The typical COP of an air source heat pump in the UK is 1.75 when producing hot water [52].
- The typical COP of a ground source heat pump in the UK is 3.16 [53].
- Thus, a value of 2 was taken as the weighted average heat pump COP, and a value of 1.5 as an average conversion factor from electricity to heat considering electrical heaters and both types of heat pump.
- Hence, 97% of households will have a conversion of 0.88 from fuel (gas/liquid/solid) to heating and 1 for direct use of electricity, while the rest of the 3% of the households will have *no* gas/liquid/solid heating, and a conversion of 1.5 from electricity to heat and 1 for direct use of electricity.

5. Results and discussion

Numerous variables are set when designing and constructing a PVT unit, and several other parameters are varied to modify its performance during operation. In the present work, two parameters were selected for careful investigation, since these significantly affect the performance and outputs of the PVT system: (i) the covering factor of the collector with PV (P) (varied between 0.2 and 1); and (ii) the cooling water flow-rate through the collector (V_P) (varied between 0.01 L/h and 200 L/h). In this section results are presented that were generated when the model described in Section 3 was run with the input parameters, variables and profiles outlined in Section 4. Firstly, in Section 5.1, a study of the performance of the PVT unit over the course of a day is undertaken, identifying the different modes of operation, after which the assessment is extended to cover a whole year in Section 5.2. This effort takes the form of parametric analyses, whose aim is to verify the influence of key parameters (P, V_P) on the overall system performance. Finally, in Section 5.3, a few selected configurations with different values of P and V_P are compared, also with respect to environmental factors (i.e. CO_2 emissions). The aim here is, by selecting the values of these parameters, to identify the most favourable configuration in terms of hot water and electricity demand coverage, whilst maximising CO_2 emission savings.

5.1. Diurnal PVT system performance

5.1.1. System operation modes

Firstly, the PVT system's operation is inspected over a typical day, for which a weekday in July is chosen. The solar irradiance, ambient conditions, hot water and electricity demands over the course of this day are taken as model inputs. In addition, an estimate of the temperature of the water in the tank (T_t) at the beginning of the day ($i = 1$) is required as an initial condition. The model is run for several days until the temperature at the beginning ($i = 1$) and at the end of the day ($i = 48$) are the same; this is found to occur when $T_t = 34.75$ °C.

Fig. 6(a) shows the daily temperature variations of the PVT unit layers, with $P = 0.75$ and $V_P = 108$ L/h. These settings were taken from previous studies (P) [19], and the manufacturer's operational specifications (V_P) [25]. It is observed that the sky temperature (T_{sky}) is significantly lower than the ambient temperature (T_a),

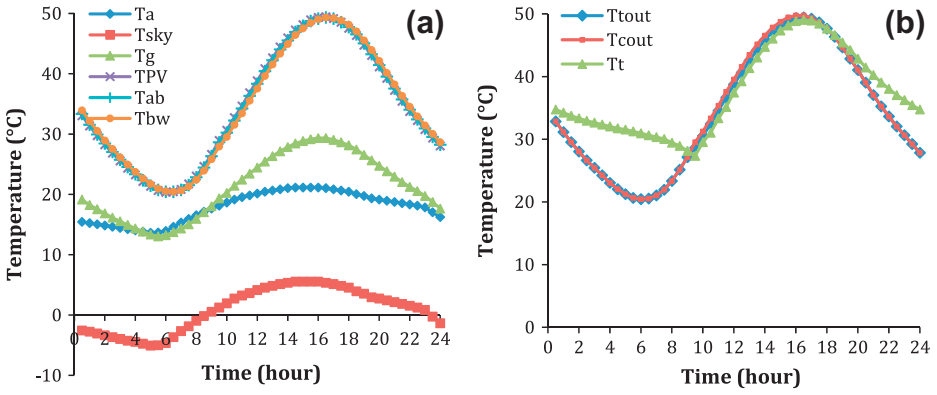

Fig. 6. Variations over the course of an average day in July of: (a) the temperatures of the different layers of the PVT unit and (b) the water storage tank temperature (T_t) and of the inlet (T_{tin}) and outlet (T_{tout}) temperatures of the heat exchanger in the tank. Results correspond to a PVT-system with a coverage factor of $P = 0.75$ and a collector cooling flow-rate of $V_P = 108$ L/h, with the value of P suggested by a previous PVT unit study [19] and the value of V_P recommended by the PVT unit's manufacturer, ENERGIES-SOL [25], respectively. N.B.: T_{PV} (cross '×' signs), T_{ab} (plus '+' signs) and T_{bw} (circles 'o') in Fig. 6(a) follow each other very closely, as expected for adjacent contacting layers, and similarly T_{tout} (diamonds) and T_{cout} (squares) in Fig. 6(b) either overlap exactly when the bypass is active (before 9 am or after 6 pm), or follow each other very closely when the bypass is deactivated (between 9 am and 6 pm) as would be expected when the flow leaving the collector enters and exits the tank at a relatively high flow-rate (as is the case shown here); refer also to Fig. 3.

leading to radiative heat transfer from the glass to the sky. As a consequence of these losses, and also the convective losses from the glass to the air due to wind, early in the day when the irradiance is near-zero (before 6 am, or $i = 12$; see Fig. 6(a)) the temperatures of all layers (glass, PV laminate, absorber) and water flow (T_{bw}) temperature decrease, with the glass temperature (T_g) eventually falling below the ambient (T_a). From 6 pm onwards there is significant solar irradiance. The temperatures of all layers gradually increase, as does the temperature of the collector cooling flow. Thus, the flow bypass valve closes (at 8:30 am, or $i = 19$; see Fig. 6(b)) and the water in the tank is heated. At dusk, when the solar irradiance falls to very low values and the ambient temperature decreases, the unit cools and the temperatures decrease, as expected.

The temperatures of the water stored in the tank (T_t) and that at the inlet (T_{cout}) and outlet (T_{tout}) of the heat exchanger in the tank (see Fig. 3) are shown in Fig. 6(b). The system model generates results as expected. Early in the day, the temperature of the water exiting the collector T_{cout} is lower than the tank temperature T_t and the system operates in bypass mode, i.e. the water is sent from the collector's outlet back to its inlet to be re-heated. The tank temperature T_t decreases due to losses and demand withdrawal. Then, from 6 am, the solar irradiance causes the temperature of the water exiting the collector, T_{cout}, to increase, and from 8:30 am, when this temperature exceeds the tank temperature T_t, the bypass valve sends the flow to the tank whose temperature starts to rise, while always remaining below that of the water exiting the heat exchanger. At the end of the day the temperature of the flow leaving the collector T_{cout} decreases due to the low irradiance; when it drops below the tank temperature T_t, the bypass is activated again so as not to cool the stored hot water.

In light of the results shown in Figs. 6 and 7, four modes can be discerned in the operation of the PVT system over the course of a day, which are crucial in devising successful control strategies for such systems:

1. For $i \leqslant 12$ (before 6 am) and $i \geqslant 36$ (after 6 pm) in Fig. 7, when there is no solar irradiance and the temperature of the PVT unit is lower than the temperature of the water entering the collector, i.e. $T_{cout} - T_{cin} < 0$: In this case it is not beneficial for the pump to be operating, thus sending the water to the collector, as the water is warming the PV module, while electricity is consumed in running the pump.

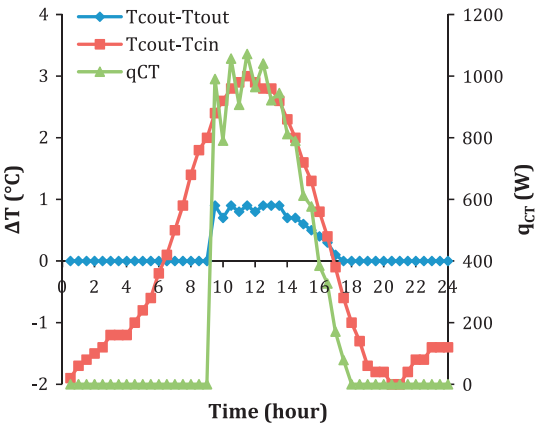

Fig. 7. Temperature rise of the water stream through the collector ($T_{cout} - T_{cin}$), temperature drop of the water stream through the heat exchanger in the hot water storage tank ($T_{cout} - T_{tout}$), and heat addition from the collector to the tank ($\dot{q}_{ct}$) over the course of an average day in July. Corresponding to the same run as the results in this figure.

2. For $13 \leqslant i \leqslant 18$ (6:30 am to 9 am) in Fig. 7, when the water temperature at the exit of the collector is higher than that at its inlet (the flow is cooling the PVT unit) yet lower than the temperature in the hot water storage tank (the flow would cool the water in the tank if it was sent there), i.e. $T_{cout} - T_{cin} > 0$ *and* $T_{cout} - T_{tout} = 0$ (or $\dot{q}_{ct} = 0$): In this case, the water pump is running and the bypass is active so the collector flow is re-circulated through the PVT unit without heat addition to the storage tank.
3. For $18 \leqslant i \leqslant 33$ (9 am to 4:30 pm) in Fig. 7, when the water temperature at the exit of the collector is higher than that at its inlet (the flow is cooling the PVT unit) and also higher than the temperature exiting the heat exchanger in the hot water storage tank (the flow is heating the water in the tank), or $T_{cout} - T_{cin} > 0$ *and* $T_{cout} - T_{tout} > 0$ (or $\dot{q}_{ct} > 0$): The pump is running with the bypass deactivated, sending the flow from the collector to the tank heat exchanger and heating the water in the storage tank.
4. For $34 \leqslant i \leqslant 35$ (5 pm–5:30 pm) in Fig. 7, when the temperature difference in the flow across the collector $T_{cout} - T_{cin}$ is smaller than the temperature difference in the tank heat exchanger $T_{cout} - T_{tout}$: In this case the bypass is again deactivated and the pump is running because, although the collector flow inlet temperature increases with time, it is still beneficial to run the system as heat is still being extracted from the collector, further heating up the water in the storage tank.

The fluctuations in the heat added to the tank $\dot{q}_{ct}$ that appear in Fig. 7, mainly in the interval 9 am–2 pm (i.e. $i = 18$–28), are due to a combination of the high demand of hot water at this time of the day (Fig. 4(b)) and the low temperature of the water in the tank (Fig. 6(b)). Due to the high demand, hot water is withdrawn from the storage tank and replaced by cold water at the lowest temperature of 10 °C, thus introducing strong fluctuations in the temperature of the water in tank and also in the heat transferred to the tank.

The corresponding electrical and thermal outputs of the PVT system throughout the day are shown in Fig. 8. Fig. 8(a) indicates that at some parts of the day when the electrical output is sufficiently high, the household demand is completely covered ($E_{neti} > 0$; squares), thus there is a surplus of electricity that can be sold to the grid. In addition, Fig. 8(b) reveals that the total domestic hot water demand (diamonds) is not completely covered at any point, however, the hot water provided by the system (squares in the plot) covers 55% of the total demand. We note that at certain times with a high solar irradiance the electrical demand also experiences significant peaks, which cannot be covered by the PVT output ($E_{neti} < 0$). During periods without solar irradiance electricity is imported, since electricity storage (batteries) is not considered in this work. It is estimated that about 82% of the electrical demand is covered with this PVT system over a day in July.

5.1.2. Model validation

Figs. 7 and 8 also serve an additional purpose, in validating our PVT unit model. At the peak irradiance of $J = 540$ W/m^2 (at around 12 noon) in the average July day, the thermal output from the system reaches a peak of approximately 1050 W (Fig. 7) and an electrical output 830 W (Fig. 8(a)) from our 15 m^2 collector array, or a thermal output of 70 W/m^2 and an electrical output 53 W/m^2. These correspond to efficiency values of 13% and 10%, respectively. Now, the electrical output of the ENERGIES-SOL PVT unit is rated by the manufacturer at 250 W$_p$ over an area of 1.62 m^2 at 1000 W/m^2 (Table A1) [16], which gives a 15% electrical efficiency. In addition, the thermal output is 867 W$_p$ for a water flow-rate of 108 L/h [16], which corresponds to a thermal efficiency of 54%, and a water temperature rise through the collector of 7 K, or a reduced temperature of $(T_{cin} - T_a)/J < 0.001$. Using a return temperature to the collector of

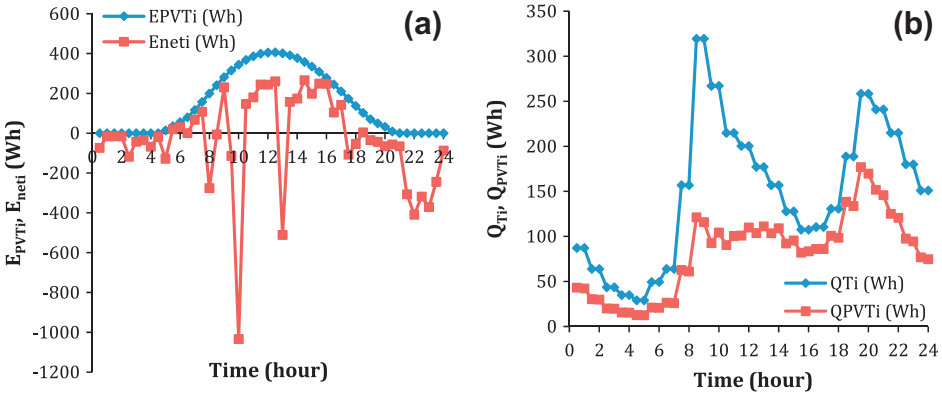

Fig. 8. Instantaneous (a) electrical and (b) thermal energy produced by the PVT system over the course of an average day in July. In (a) showing total production and net production after accounting for the household demand. In (b) showing total household demand (from Fig. 4(b)) and production by the PVT system. Energies shown here over a 30-min time step. Corresponding to the same run as the results in Figs. 7 and 8.

60 °C at $J = 540$ W/m^2, we would expect $(T_{cin} - T_a)/J = (60 - 25)/540 = 0.065$ during July operation. From a typical thermal efficiency performance curve for a sheet-and-tube PVT/water collector [54], the thermal efficiency is expected to be within the range ~10–15%.

5.1.3. Effect of collector flow-rate

The average solar irradiance over the entire year was calculated, and the month with the closest average irradiance was selected as an *average month*, which for London was found to be March. For this month, the collector flow-rate V_P was varied from zero (no water flow through the collector) to 200 L/h, with higher resolution in the range 0–40 L/h, while the covering factor was set to 0.75 as suggested in Ref. [19], and as employed previously in Figs. 6–8. Fig. 9(a) shows that the hot water demand covered, $DC_{HW,}$ exhibits a significantly greater sensitivity to the collector flow-rate V_P, compared to the electrical demand covered DC_E. The hot water demand covered DC_{HW} has an optimum at around 10–20 L/h. On the other hand, on closer inspection of the electrical demand covered DC_E (Fig. 9(b)) it is observed that the optimum value of collector flow-rate V_P that provides the maximum electricity can be found between 60 and 120 L/h, although it should be noted that the range of variation is much smaller than that for the hot water coverage (2% vs. 30%).

It is possible to explain the slight differences in the variations of the hot water and electrical demands covered. When there is no water flow through the collector the demand covered DC_{HW} is zero. As the collector flow-rate V_P is gradually increased, the covered demand similarly increases, yet at high flow-rates the temperature reached at the outlet of the collector is low, such that it cannot

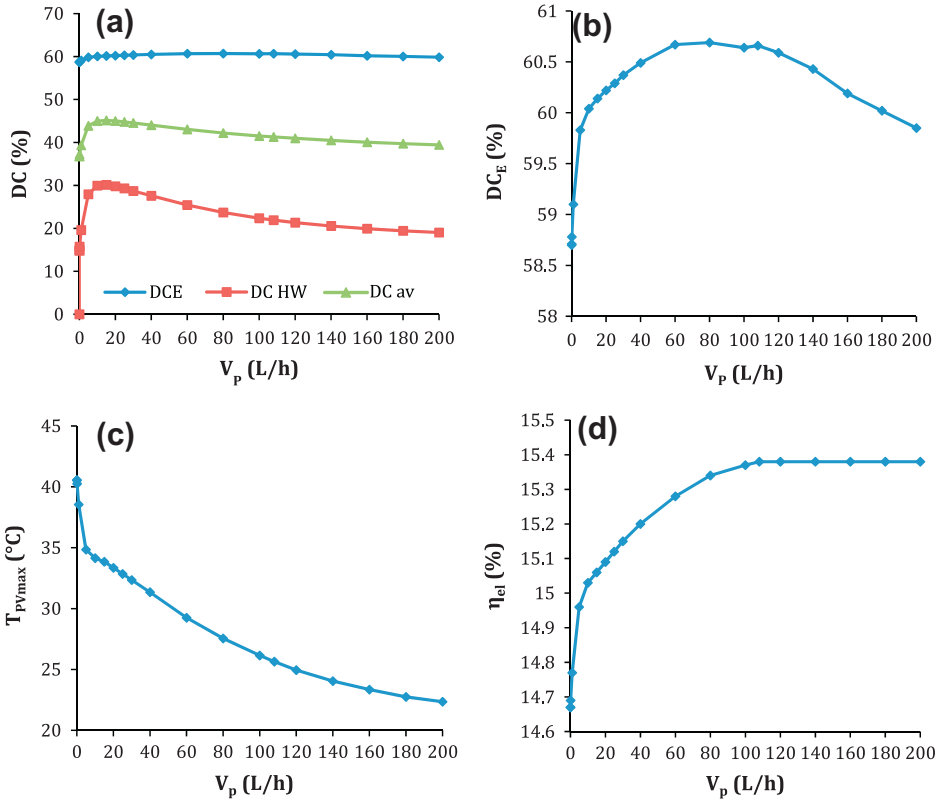

Fig. 9. (a) Electrical, hot water and average demand covered, (b) electrical demand covered, (c) maximum temperature of the PV and (d) average PV module efficiency over a weekday in the average month (March) for 75% covered ($P = 0.75$) PVT systems with different collector flow-rates V_P.

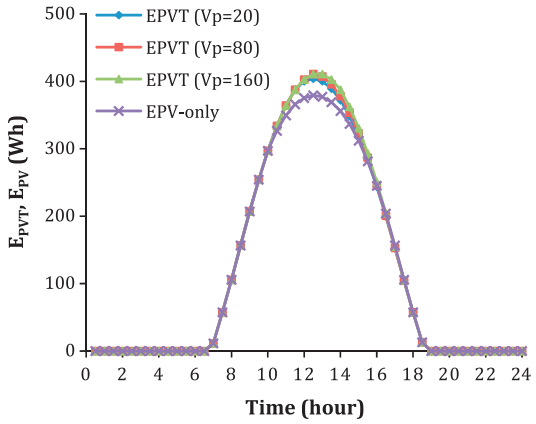

Fig. 10. Electricity generated over the course of a day in the average month (March) by fully-covered ($P = 1$) PVT systems with collector flow-rates $V_P = 20$, 80 and 160 L/h, and comparison with the PV-only system.

be used to heat the water in the storage tank, so the hot water demand coverage decreases again. The variation in the electrical demand covered DC_E can also be explained in terms of a combination of factors. At intermediate collector flow-rates V_P (around ~100 L/h), the maximum PV module temperature T_{PVmax} is low (Fig. 9(c)), which allows a high PV module efficiency η_{el} of 15.3–15.4% (Fig. 9(d)) and a correspondingly high electrical demand coverage (Fig. 9(b)). However, at even higher collector flow-rates, the PV efficiency is not further enhanced and displays a degree of saturation, yet the energy required to drive the collector pump is now higher, and the improvement in the PV efficiency does not offset the penalty of running the pump. Therefore, the covered electrical demand decreases again.

5.1.4. Comparison with a PV-only system

Fig. 10 shows the energy produced throughout a day in the average month (March) for a PVT system with three different collector flow-rates, V_P, and for a PV-only system. The maximum energy produced by the PVT system increases beyond that of the PV only unit, although the differences among the PVT configurations studied are small. This is important, as together with Fig. 9 it suggests that the increase in the electricity produced at high collector flow-rates ($V_P = 160$ L/h) may not compensate the decrease in the hot water demand covered. It is concluded that the collector flow-rate affects strongly the overall hot water and electrical delivery performance of the PVT system and its effect should be studied over a complete year.

5.2. Annual parametric analyses

5.2.1. Nominal PVT arrangement

With the role of the collector flow-rate (V_P) clarified, a series of parametric analyses can be undertaken over an entire year of operation. The aim here is to select appropriate values for both P and V_P that maximise the electrical (DC_E) and hot water (DC_{HW}) demands covered, while maximising the CO_2 emissions savings. The results from this effort are shown in Figs. 11 and 12. It is observed, once again, that the covered electrical demand is not notably affected (<5% variation) by changes to the collector flow-rate, V_P, whereas the covered hot water demand is significantly affected, decreasing by ~35% as V_P increases from 20 L/h to 200 L/h. This is due to the low collector temperatures reached at higher V_P, therefore requiring a greater use of the auxiliary heater to supply the hot water at 60 °C to the house. On the other hand, the electrical output of the PVT system increases linearly with the increase in P (Fig. 11(b)), due to the proportionally larger surface area of the PV module. However, as the PV module area increases, there is less absorber

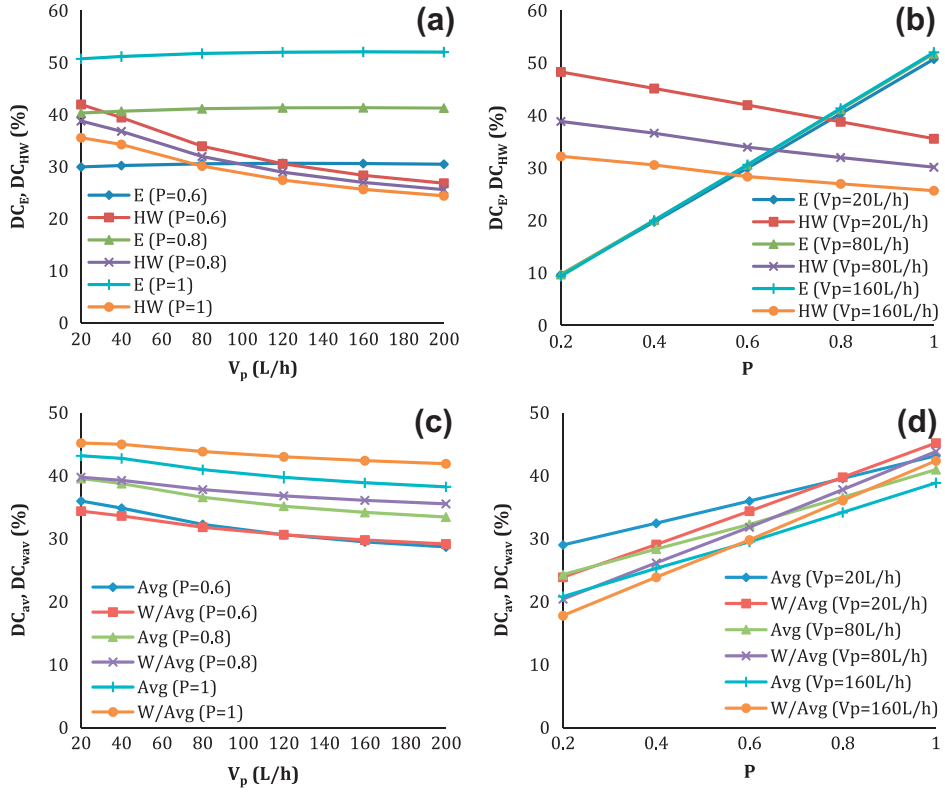

Fig. 11. For selected PVT configurations: (a) electrical and hot water demand covered over a year for different values of V_P and (b) for different covering factors, P. (c) Average and weighted average demand covered over a year for different values of V_P and (d) for different covering factors, P.

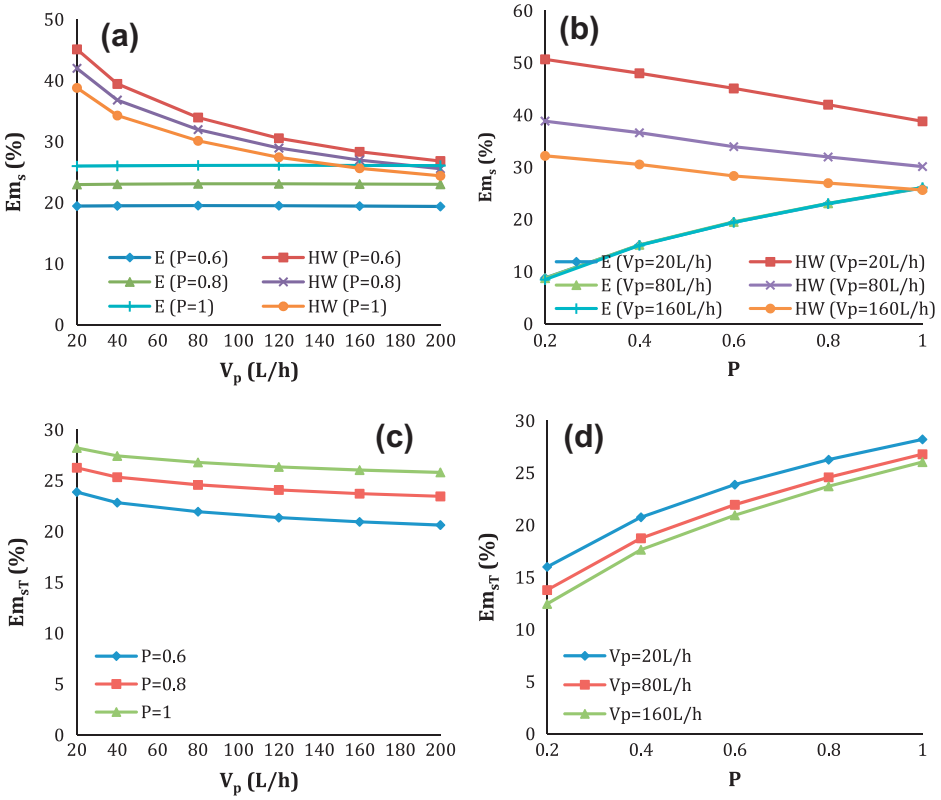

Fig. 12. For the same selected PVT configurations in Fig. 11: (a) separate contributions towards CO_2 emission savings due to electricity and hot water production over a year for different values of V_P and (b) for different covering factors, P. (c) Total CO_2 emission savings from both electricity and hot water production over a year for different values of V_P and (d) for different covering factors, P.

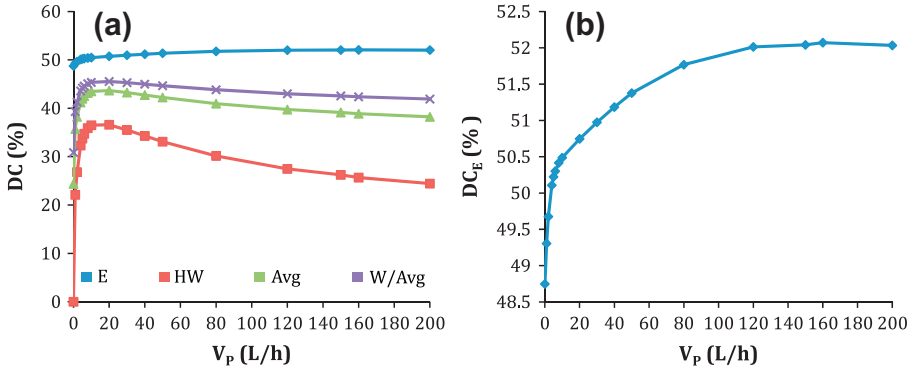

Fig. 13. (a) Percentage of electrical (E), hot water (HW), average (Avg) and weighted average (W/Avg) demand covered and (b) electrical demand covered throughout the year for different values of V_P for a PVT system completely covered by PV ($P = 1$; i.e. the total surface area of the solar collector is covered entirely by the PV laminate).

plate area directly exposed to the solar irradiance (which has a higher absorptivity than the PV laminate), so the heat transferred to the water flowing through the PVT collector decreases, diminishing the amount of hot water demand covered. Together, the results indicate that high covering factors P are desirable in order to maximise the electrical output, although the hot water production decreases, but to a smaller extent.

One can conclude that the collector flow-rate V_P does not strongly influence the electrical output, but it does affect the hot water output, while the covering factor P affects the electrical output considerably more than it does the thermal equivalent. Thus, and from the average/combined measures of demands covered in Fig. 11(c) and (d), one can suggest high coverage values ($P = 0.8$–1) and the use of low flow-rates ($V_P = 20$–80 L/h) as being appropriate in terms of adequately covering both the electrical and thermal demands.

Fig. 12 indicates that the CO_2 emission savings due to PVT hot water production are more significant than the equivalent emission savings due to electricity production. Nevertheless, the *total* percentage of emission reductions is more sensitive to the electrical than the thermal emissions, due to the fact that the contribution of electricity generation towards the total emissions is higher than that associated with hot water production. Furthermore, while the electrical emission reductions do not vary appreciably for different V_P, the emission reductions due to hot water production decrease strongly as V_P increases, due to the lower amount of net heat added to the tank, which means that more auxiliary heat is required. Therefore, low collector flow-rates can

achieve a higher percentage of total emission savings. The emissions savings due to PVT electricity production increase as the covering factor P increases, while those due to hot water production decrease. Still, since the CO_2 emissions due to electricity production are significantly larger than those for hot water production, the total emission reductions follow the electrical trend, suggesting the use of high covering factors.

It can be concluded, both from an electrical and thermal delivery perspective and with regards to emissions, that high covering factors P and low collector flow-rates V_P are recommended for our PVT system. In order to observe closely the PVT performance at low flow-rates, a more detailed parametric analysis was performed in which the flow-rate was varied down to very low values, over the full range 0–200 L/h, for a covering factor of 1. Fig. 13 shows that the collector flow-rate that maximises the hot water demand covered is 20 L/h, while the electrical demand covered is maximised at 160 L/h. However, the range of variation of the latter is much smaller than the former, and as a consequence the collector flow-rate that maximises both the average and weighed average demand covered is 20 L/h (highlighted as bold and italic in Table 1).

5.2.2. Variations in the PVT system configuration

The results from the parametric analysis demonstrated that high covering factors P and low collector flow-rates V_P are preferable in maximising the coverage of electricity and hot water demands throughout the year, while at the same time maximising the CO_2 emissions savings. In order to gain insight into the detailed combined performance of the PTV system throughout the year, five combinations of collector covering factors and flow-rates are selected, and considered in detail in this section:

- System featuring a high electrical performance unit design, operated for a high electrical output: Covering factor $P = 1$ and collector flow-rate $V_P = 160$ L/h.
- System featuring a high electrical performance unit design, operated for a high thermal output: Covering factor $P = 1$ and collector flow-rate $V_P = 20$ L/h.
- System featuring a high thermal performance unit design, operated for a high thermal output: Covering factor $P = 0.6$ and collector flow-rate $V_P = 20$ L/h.
- System featuring a high thermal performance unit design, operated for a high electrical output: Covering factor $P = 0.6$ and collector flow-rate $V_P = 160$ L/h.
- Intermediate solution system: Covering factor $P = 0.8$ and collector flow-rate $V_P = 80$ L/h.

The first combination was chosen to represent a system with a PVT unit that exhibits the best electrical performance (high P), operated so as to maximise its electrical output (high V_P), and the second combination is the same system operated to maximise its thermal output (low V_P). Similarly, the third combination represents a system with a PVT unit that exhibits the best thermal performance (low P), operated so as to maximise its electrical output (high V_P), and the fourth is the same system operated to maximise its electrical output (low V_P). The final combination is an intermediate solution in terms of design and operation.

Fig. 14(a) shows that the electrical production per month follows a profile similar to the solar irradiance, with a more than 3 times higher output in the summer compared to the winter. It is also possible to conclude that the units with covering factor equal to unity produce significant more electrical output than the PVT units with lower covering factors in summer months. Yet, there is little difference between the electrical outputs of the systems with different collector flow-rates. The net power imported or exported by the house in each month (Fig. 14(b)) shows similar results. The net electrical output varies significantly depending on the month, also given the higher electricity demand in winter months when the PVT electrical output is also lower, thus requiring more energy to be bought from the grid (negative values of E_{PVTnet}). It should be noted that for PVT units with $P < 1$, the net energy is always negative, which means that electricity is always be bought from the grid at the end of each month, while for $P = 1$, the total net energy per month is positive during the summer months, when electricity can be sold to the grid, generating revenue for the household.

In terms of hot water production (Fig. 14(c)), both the covering factor and the collector flow-rate influence the output of the system. The best results throughout the year are found with a covering factor of 0.6 and a 20 L/h collector flow-rate, while the worst results are given when a covering factor of 1 and a collector flow-rate of 160 L/h is considered. Hence, it can be concluded that the slight improvement in electrical output at higher flow-rates observed in relation to Fig. 14(a) and (b) may not outweigh the decrease in hot water production.

Finally, in terms of CO_2 equivalent emissions, the emissions associated with electricity production are always greater than those associated with hot water (Fig. 15). Depending on the configuration considered, both vary by up to 10–15 $kgCO_2$ per month, with a greatest deviation in the summer and smallest in the winter.

5.3. Overall assessment and comparison with a PV-only system

In this section the PVT configurations selected above are compared with each other as well as with a PV-only system in terms of demand covered and CO_2 emissions saved over the lifetime of the PVT system, considering two different lifetimes (n), 20 years [11] and 25 years [55]. The results of this comparison are summarised in Fig. 16 and Table 2. Table 2 shows that a complete coverage of the collector with PV is preferred in terms of electrical, average and weighted average demand covered, as well as in terms of the total CO_2 emissions saved, whereas the lowest coverage factor ($P = 0.6$) has the highest thermal output and thermal demand covered. Still, the thermal output of the fully covered 'high electrical performance' PVT system can be significantly increased (by >40%) by using a lower collector flow-rate V_P if this is desired from the household, which can be achieved in a practical system with the use of a variable-flow pump, whereas the electrical output of the 'high thermal performance' system only marginally improves (by ~5%) by increasing the cooling flow from $V_P = 20$ L/h to 160 L/h. Fig. 16 confirms that a high P (=1) and a high V_P in the PVT collector are preferred for maximising the covered electrical demand, which allows a slightly higher electrical output than the PV-only system. However, the hot water demand covered decreases strongly at high

Table 1
Percentage of electrical, hot water, average and weighted average demand covered for different collector flow-rates for a PVT system completely covered by PV ($P = 1$). Maximum values highlighted as bold and italic.

V_P (L/h)	**0**	**1**	**2**	**4**	**5**	**6**	**8**	**10**	***20***	**30**	**40**	**50**	**80**	**120**	**150**	***160***	**200**
DC_E	48.75	49.31	49.68	50.11	50.22	50.30	50.42	50.49	50.75	50.97	51.18	51.38	51.77	52.01	52.04	***52.07***	52.03
DC_{HW}	0.00	22.11	26.81	32.30	33.74	34.73	35.90	36.50	***36.60***	35.52	34.30	33.10	30.16	27.47	26.23	25.68	24.43
DC_{av}	24.37	35.71	38.24	41.20	41.98	42.52	43.16	43.49	***43.67***	43.25	42.74	42.24	40.96	39.74	39.14	38.88	38.23
DC_{wav}	30.85	39.32	41.28	43.57	44.17	44.59	45.09	45.35	***45.55***	45.30	44.98	44.67	43.83	43.00	42.57	42.38	41.90

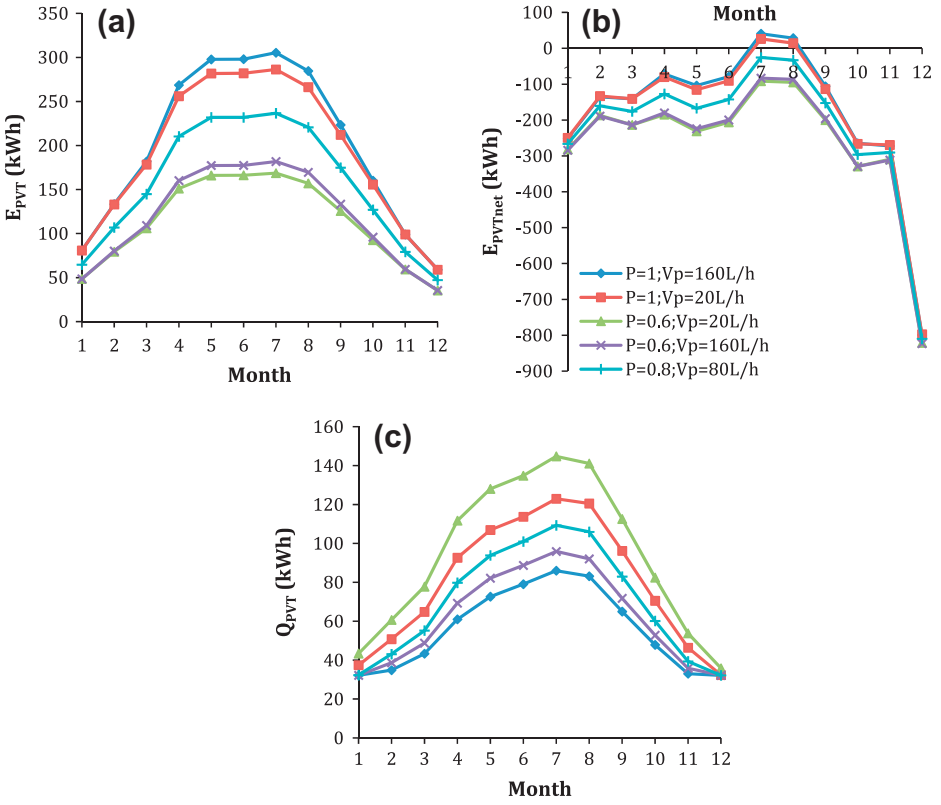

Fig. 14. (a) Total energy produced by the PVT unit, (b) net energy imported/exported by the house per month and (c) thermal energy produced by the PVT unit per month, for selected PVT configurations. All figures have the same legend as in (b).

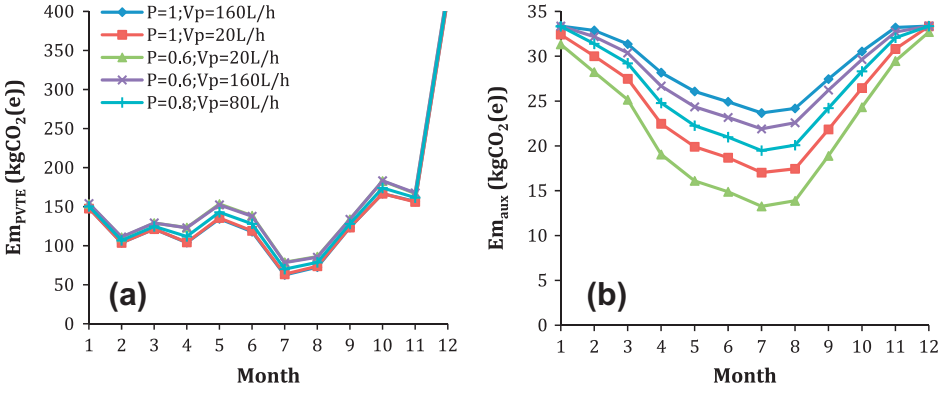

Fig. 15. CO_2(e) emissions due to (a) power and (b) hot water consumption per month, for selected PVT configurations. Legend relates to both plots. Both figures have the same legend as in (a).

V_P, while the improvement in the electrical output is only minimal compared to lower V_P; therefore the best compromise seems to be a collector flow-rate of V_P = 20 L/h, with which 50.7% and 35.6% of the electrical and hot water demands, respectively, are covered over the course of a full year (see Table 2). Finally, this is also the best configuration in terms of CO_2 emissions reduction, as 16 tonnes of CO_2 can be saved over a lifetime period of 20 years, compared to the 11.8 tonnes of CO_2 saved with a PV-only system of the same capacity. Importantly, all selected PVT configurations outperformed the PV-only system in terms of emissions, by up to 36% in the best PVT case.

5.4. Brief economic considerations

At this stage, it is important to perform a brief economic analysis relating to the deployment of the proposed PVT systems in the UK domestic sector. A number of representative configurations where selected for this purpose, with collector flow-rates: (i) V_P = 20 L/h, (ii) V_P = 40 L/h, (iii) V_P = 80 L/h, and (iv) V_P = 160 L/h, all with a fully covered PVT collector, P = 1, since it is found in the present work that this is the most economically beneficial configuration for the chosen application of this technology. The initial/capital expense was estimated by summing the individual costs of all system components, which in all cases was found to amount to £8500 for a 2.25 kW_p (electrical) PVT system with a 150 L hot water storage tank, including (in addition to the PVT collector and tank) the inverter, pump, structural supports, piping, wiring, installation, etc. After accounting for the running costs of conventional equivalents (buying electricity from the grid and natural gas for a modern high-efficiency boiler) and any income from the currently available incentives, i.e. (i) the Feed-in Tariffs (FITs); (ii) the Renewable Heat Premium Payment (RHPP); and (iii) the

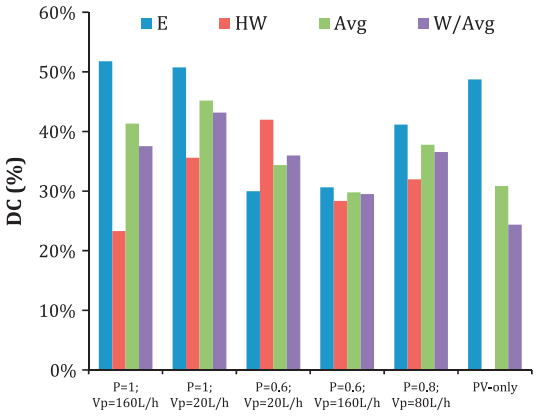

Fig. 16. Percentage of electrical (E), hot water (HW), average (Avg) and weighted average (W/Avg) demand covered for selected PVT configurations and comparison with the PV-only system.

Renewable Heat Incentive (RHI), which is expected to become available to the UK domestic sector shortly, it was found that the payback periods of the PVT systems ranged from 10 to 12 years, also depending on the discount (2.5–10%) and inflation rates (3.2–6%) used in the calculation. The following data was used in arriving at these estimates: (i) an electricity price of 17.4 p/kW h; (ii) a natural gas price of 5.8 p/kW h; (iii) a FIT payment for PV of 43.3 p/kW h; (iv) a one-off £300 RHPP voucher for the installation of a solar-thermal product; and (v) a RHI payment of 8.5 p/kW h, all for the specific case of the UK. The PVT system payback periods were compared with an equivalent 2.25 kW_p PV-only system, which was evaluated by using an identical approach. The payback period of the PV-only system was found to be approximately 7 years at current levels and means of support, although it is noted that this can only cover an electrical demand, as opposed to a PVT system that can cover this as well as a demand for hot water. Generally, the selected PVT systems were found to be very closely matched in our assessment, with the $V_P = 20$ L/h configuration showing a marginally lower payback.

6. Further discussion and conclusions

The current market for both solar thermal and PV systems is experiencing significant growth, owing to the recognition of these technologies as key and necessary measures for sustainable energy provision and carbon mitigation [4]. This growth can be attributed to incentives derived from government policy support and the increasing environmental awareness of the end-user. Consequently, the integration of these solar-based technologies to form a hybrid PVT system has considerable potential in this scenario, not only in combining the advantages of the separate units into a single system able to provide both electricity and hot water, but also in the synergistic manner in which the heat removal for hot water provision cools and increases the efficiency of the PV cell. Therefore, a similar growth in the demand for PVT systems is expected, with the domestic sector almost certainly forming the largest market share (currently ~90% of the market according to Ref. [14]). Policy-makers have a crucial role to play in boosting the uptake of these technologies by means of establishing them as cost-competitive and commercially attractive alternatives to conventional solutions [4].

The present effort focuses on the performance of PVT/water systems in the domestic sector, in order to examine their suitability for the distributed generation of electricity and simultaneous provision of hot water in this application. Different solar-thermal collector configurations were reviewed in a number of excellent previous studies [8–11,15,22]. These studies concluded that the sheet-and-tube configuration is a highly appropriate option in terms of both electrical and thermal efficiency, and also that this is the easiest and most affordable configuration to manufacture as it relies on well-known, readily available technology. In addition, mono-crystalline (c-Si) PV cells are often selected by reason of their higher electrical output (efficiency), as well as their greater stability compared to both amorphous and poly-crystalline module counterparts. All commercially available PVT units that have been identified in the present study employ c-Si.

In hybrid PVT systems the total energy output (electricity plus heat) depends on several factors and typically there is a conflict between the electrical and thermal performance [8,10,12,15]. The present study has investigated two key system parameters that strongly influence the output of the PVT system: the cooling flow-rate through the collector unit; and the covering factor of the solar collector with PV cells [21]. The aim was to maximise the supply of both electricity and hot water in the particular scenario of an average 3-bedroom terraced house in London, UK [42], while also maximising the total CO_2 emission savings. To the best knowledge of the authors the novelty of the present effort arises from it being the first UK-based effort of its kind, following on from excellent investigations of other configurations and in other geographical regions, such as in Refs. [56–58]. Of particular interest in the present work has been the consideration of the whole system (PVT unit, hot water storage tank, auxiliary heater and the household), with varying daily temporal profiles of solar irradiance and household demands, over the course of an entire year, including a parametric analysis and attempt to identify better-performing configurations and operating conditions/strategies.

The main findings regarding the covering factor are: (i) that it significantly influences the electrical output, such that the percentage of electrical demand covered increases notably with the covering factor, while it only has a minimal effect on the thermal output; and (ii) that the total CO_2 emissions savings are more affected by the electrical output, due to the fact that emissions associated with electricity generation are much higher than those associated with hot water production. On the other hand, the main findings

Table 2
Summary of the performance and the environmental assessment for selected PVT configurations and comparison with the PV-only system. Maximum values highlighted as bold and italic.

			$P = 1$; $V_P = 160$ L/h	$P = 1$; $V_P = 20$ L/h	$P = 0.6$; $V_P = 20$ L/h	$P = 0.6$; $V_P = 160$ L/h	$P = 0.8$; $V_P = 80$ L/h	PV-only
E_{PVT} (kW h)			***2392***	2290	1355	1428	1876	2193
Q_{PVT} (kW h)			670	955	***1127***	740	835	0
DC_E (%)			***51.8%***	50.7%	30.0%	30.6%	41.2%	48.7%
DC_{HW} (%)			23.3%	35.6%	***42.0%***	28.4%	32.0%	0.0%
DC_{av} (%)			37.5%	***43.2%***	36.0%	29.5%	36.6%	24.4%
DC_{wav} (%)			41.3%	***45.2%***	34.4%	29.8%	37.8%	30.9%
Em_{sT} (kg CO_2(e)/yr)			740	***800***	688	607	709	589
Tonnes CO_2 saved	***n***	**20**	14.8	***16.0***	13.8	12.1	14.2	11.8
	n	**25**	18.5	***20.0***	17.2	15.2	17.7	14.7

with regards to the collector cooling flow-rate are: (i) that the percentage of hot water demand covered is considerably more sensitive than the electrical demand covered to the increase in the collector flow-rate, with the former decreasing at higher flow-rates; and (ii) that the emissions savings that arise from the hot water output are affected by the increase in the collector flow-rate (due to the increase in auxiliary heat at higher the collector flow-rates), but the total CO_2 emissions savings are not significantly affected by this parameter. Consequently, high covering factors and low collector flow-rates are suggested. With these findings in mind, it can be concluded that the investigated parameters influence strongly the electricity and hot water production, with the former being more sensitive to covering factor variations, and the latter to collector cooling flow-rate variations. Similar results were found when five selected PVT configurations were investigated throughout the different months of the year. Specifically, a covering factor in the range $P = 0.8–1$ and the use of low collector flow-rates in the range $V_P = 20–80$ L/h are recommended in order to maximise the overall coverage of the demanded heating and power throughout the year while increasing the total CO_2 emissions savings.

Up to 52% of the total annual electrical demand (for a configuration with $P = 1$, $V_P = 160$ L/h) and up to 48% of the annual hot water demand (for a configuration with $P = 0.2$, $V_P = 20$ L/h) could be covered by such a PVT system. The most suitable configuration ($P = 1$ and $V_P = 20$ L/h) was selected for direct comparison with a PV-only system consisting of c-Si modules with the same peak capacity as the PVT system (2.25 kW_p). The results indicate that a larger amount of the annual electricity demand is covered by the PVT unit (51% vs. 49%), while also covering 36% of the total demand for hot water. Consequently, the CO_2 emissions are substantially lower (16 tonnes of CO_2 saved vs. 11.8 tonnes, over a lifetime period of 20 years). All investigated PVT configurations outperformed the PV-only system in terms of emissions. A surplus of electricity can occur with some PVT configurations during the summer months, and this is exported to the grid. The improved capacity of the PVT technology to cover the total (both electrical and thermal) domestic energy needs and much greater potential for emissions abatement compared to PV-only systems does come a higher cost, with payback periods estimated in the range 10–12 years compared to 7 years for PV. This of course is a strong function of current UK incentives. We suggest that there is a need to consider these more carefully in the light of present results.

In summary, we conclude that the configuration of the PVT system significantly affects its thermal and electrical output, and because is not possible to maximise both outputs at the same time, the values chosen for the main system parameters depend on the specific end-user needs. On the basis that the CO_2 emissions of electricity are significantly higher than that of natural gas, the electricity production is usually the priority. In the specific case of the UK where the temperatures reached in the PVT unit are not too high, it is recommended to completely cover the solar collector with PV, since the loss in electrical efficiency is more than offset by the higher electrical output allowed by larger PV surface area. In addition, a low collector flow-rate is recommended. However, one should consider that in other geographical locations with higher solar irradiance it may be necessary to reconsider the preferred covering factor as well as the collector flow-rate.

This paper has focused mainly on the technical performance of a hybrid PVT/w system in a domestic setting in the UK with only a brief consideration of costs, which are expected to affect uptake decision-making, for example owing to the higher up-front investment costs required by PVT systems compared to standard PV-only systems. Therefore, a more in-depth complementary economic study may also be required for a complete assessment of the suitability of these systems and for a better understanding of the current effects of government incentives. When strong incentives, such as FITs, are applicable (as is the case currently in the UK) there is an added benefit in producing surplus electricity because a household featuring a PVT or PV system can then export this electricity and generate an income, thus making the system more attractive.

Acknowledgement

This work was supported by the Research Councils UK (RCUK) [grant number EP/E500641/1].

Appendix A. PVT system parameters

The PVT system evaluated in this paper is based on the commercially available hybrid unit ENERGIES-SOL [16]. Many technical specifications required for the modelling of this system, though not all, are available in the specifications sheet provided by the manufacturer. The rest of the required parameters have been estimated from the literature [3,22,24,30,31]. The total roof area available in an average terraced house in London is about 15 m^2 [44]. Since the total area of a single PVT module is 1.62 m^2, the system considered consists of 9 modules arranged and operating in parallel. The module consists of mono-crystalline (c-Si) cells, which provide a high module efficiency of 15.4% at Standard Test Conditions (STC: 1000 W/m^2 and 25 °C). The temperature coefficient for the PV module, β_0 (used in relation to Eq. (6)), is 0.0053 K^{-1}. The complete PVT system has a nominal electrical power of 2.25 kW_p, with each module contributing an equal 250 W_p of nominal electrical power. Important technical specifications are detailed in Table A1.

The manufacturer does not provide details of the design and materials used, such the optical and thermal properties of the different layers and their geometrical specifications. These parameters are important in determining the performance of the PVT unit and are required in the energy balances developed in Section 3 to evaluate the system. The values used in this paper of the optical and thermal properties of the different materials from which the PVT unit is constructed where taken from the literature [3,22,24,26,30,59,60] (see Table A2). Similarly, to calculate the convective heat transfer to the cooling water stream flowing through the collector, it is necessary to know the geometry of the riser tubes. As this information is not provided, it has also been estimated from values found in literature for similar systems [3,22,24] (also stated in Table A2).

Once the geometry of the riser tubes is selected, it is possible to estimate the convective heat transfer coefficient of the water flowing through the collector. However, it should be kept in mind that this coefficient also depends on the water flow-rate through the collector. Initially, the recommended water flow-rate by the

Table A1
Technical specification of the modelled PVT unit (single module) [17].

Nominal power	250	W_p
Total surface area	1.624	m^2
Total aperture area	1.566	m^2
Voltage at Maximum Power Point (MPP)	30	V
Current at MPP	8.34	A
Open circuit voltage	36.9	V
Short circuit current	8.34	A
Pressure drop at the recommended flow-rate	150	mbar
Maximum operating pressure	3.5	bar
Recommended flow-rate	108	L/h
Reference PV module efficiency	15.4	%
Temperature coefficient of cell power (β_0)	0.53	%/K
Normal Operating Cell Temperature (NOCT)	45 ± 0.2	°C
Type of solar cell	Mono-crystalline (c-Si)	

Table A2
Optical and thermal properties, thicknesses, geometrical characteristics, and other parameters related to the different layers that compose the modelled PVT unit.

Layer	Parameter/variable		Value	Refs.
Glazing	A	Aperture area (m^2)	1.566	[16]
	δ	Thickness (m)	0.0032	[16,22,24]
	ε	Emissivity	0.88	[3,26,28]
	τ	Transmittance	0.9	[31]
	ρ_d	Diffuse reflectance	0.16	[33]
Air layer	δ	Thickness (m)	0.005	
	k	Thermal conductivity (W/m K)	0.025	[22]
PV plate	A_{PV}	Area of the cell		
	P	Covering factor	0.75	
	ρ	Packing factor	0.9	[60]
	α	Absorptivity	0.9	[59]
	ε	Emissivity	0.9	[22]
	δ	Thickness (m)	0.00035	[24]
EVA	δ	Thickness (m)	0.0005	[22,30]
	k	Thermal conductivity (W/m K)	0.35	[22,30]
Adhesive	δ	Thickness (m)	$5{\cdot}10^{-5}$	[22,30]
	k	Thermal conductivity (W/m K)	0.85	[22,30]
PE-Al-Tedlar layer	δ	Thickness (m)	0.0001	[22,30]
	k	Thermal conductivity (W/m K)	0.2	[22,30]
Absorber plate	α	Absorptivity	0.95	[3]
	ε	Emissivity	0.05	[3]
	δ	Thickness (m)	0.0002	[3,24]
	k	Thermal conductivity (W/m K)	310	[3]
Riser tubes	D	Diameter of tube (m)	0.01	[22,24]
	N	No. of tubes	11	[3,22]
	W	Spacing of tubes	0.095	[22]
Insulation	δ	Thickness (m)	0.02	
	k	Thermal conductivity (W/mK)	0.035	[3,22,33]

manufacturer (ENERGIES-SOL) was considered and a value of 259 W/m^2 K was found. However, it should be noted that the manufacturer-recommended cooling flow-rate varies significantly across different commercial PVT units, and also in the literature. In Ref. [40] the collector flow-rate is 40 L/m^2 h, whereas Refs. [26,27] suggest 50 L/m^2 h. While these values are similar, they differ significantly from the manufacturer-recommended flow-rate for our selected PVT unit, which is 108 L/h or around 70 L/m^2 h [16]. Other studies consider a much wider range of flow-rates [30], stating that the optimum flow-rate lies between 18 L/h and 270 L/h. Therefore there is a lack of agreement concerning the recommended or optimum flow-rate, which will depend strongly on the specific needs of the particular application. As a consequence, this work considers explicitly the effect of the water flow-rate through the collector on the overall performance of the system.

Another necessary parameter that is required is the pump (hydraulic) power required to drive the collector closed-loop water-cooling circuit. The recommended flow-rate provided by the PVT manufacturer has been used as an initial value of the pumping power, in order to select a suitable pump among those available in the market, for which a full pump curve was obtained. The pump specifications are summarised in Table A3.

Therefore, the values of the convective heat transfer coefficient of the cooling flow through the collector and of the pumping power are explicitly calculated in the model, once the collector flow-rate has been imposed.

Table A3
Water pump and collector cooling circuit specifications [61].

H_T	Total head loss through the system	2.91	m
Q	Nominal flow-rate	0.972	m^3/h
	Operating pressure	3.5	bar
P_P	Nominal electrical consumption	9.07	W
Q_{max}	Maximum flow-rate	4	m^3/h
H_{Tmax}	Maximum head	6	m
	Maximum operating pressure	10	bar
η_P	Pump efficiency	0.85	–

Appendix B. Water storage tank parameters

The daily hot water demand for the house studied is about 122 L, so a water storage tank with a capacity of 150 L was selected. To estimate the heat transferred from the collector to the water contained in the tank, the overall heat transfer coefficient of the heat exchanger immersed in the tank should be calculated, for which the dimensions of this heat exchanger are required. Table B1 summarises the parameters used. An overall heat transfer coefficient $(UA)_t$ of 573 W/K is found based on these values. For different collector flow-rates the model automatically calculates the new number of transfer units NTU and heat exchanger effectiveness ε.

Table B1
Summary of the main parameters of the water storage tank and the immersed heat exchanger.

M_t	Storage tank capacity (kg)	150	[31]
H_t	Height of the tank (m)	1.5	[31]
D_t	Diameter of the tank (m)	0.36	[31]
S_t	Surface area of tank (m^2)	1.9	[31]
U_t	Overall heat loss coefficient (W/m^2)	3	[31,62]
$(UA)_t$	Overall heat transfer coefficient (W/K)	573	
NTU	Number of transfer units	0.51	
ε	Heat exchanger effectiveness	0.4	

There are also some heat losses through the storage tank walls, which are accounted for in the present work. An overall heat loss coefficient for the storage tank, U_t, was taken from the literature. The values found in literature are very similar, so a value of $U_t = 3$ W/m^2 is used [31,62].

Table B2
Initial conditions and other important constant system parameters.

T_{win}	Mains water temperature	10	°C
T_t ($i = 0$)	Initial temperature of water storage tank	34.75	°C
T_{cin} ($i = 0$)	Initial temperature of water flowing through the collector	34.75	°C
T_{as}	Average ambient temperature in the house (tank surroundings)	20	°C
h_w	Convective heat transfer coefficient of water flow through the collector	259	W/m^2 K

Finally, initial conditions are required at the beginning of the day ($i = 1$) for the solution of the equations. These include the initial temperature of the water stored in the tank and the initial temperature of the water entering the collector. In addition, two further parameters must be defined, which are the mains water temperature entering the storage tank, and the average ambient temperature in the house (T_{as}) that is required to estimate the losses through the storage tank walls (which is located inside the house) (see Table B2).

References

[1] Markides CN. The role of pumped and waste heat technologies in a high-efficiency sustainable energy future for the UK. Appl Therm Eng 2013;53:197–209.
[2] House of Lords. The EU's target for renewable energy: 20% by 2020. European Union Committee. 27th Report of Session 2007–08. 2008; Volume I: Report.
[3] Bhattarai S, Oh J, Euh S, Kafle GK, Kim DH. Simulation and model validation of sheet and tube type photovoltaic thermal solar system and conventional solar collecting system in transient states. Solar Energy Mater Solar Cells 2012;103:184–93.
[4] Chi-Jen Y. Reconsidering solar grid parity. Energy Policy 2010;38:3270–3.
[5] Ekins-Daukes NJ. Solar energy for heat and electricity: The potential for mitigating climate change. Graham Institute for Climate Change; 2009. Briefing paper No. 1.
[6] Bagge H, Johansson D. Measurements of household electricity and domestic hot water use in dwellings and the effect of different monitoring time resolution. Energy 2011;36:2943–51.
[7] Chow TT. A review on photovoltaic/thermal hybrid solar technology. Appl Energy 2010;87:365–79.
[8] Tripanagnostopoulos Y, Nousia T, Souliotis M, Yianoulis P. Hybrid photovoltaic/thermal solar systems. Sol Energy 2002;72:217–34.
[9] He W, Chow T, Ji J, Lu J, Pei G, Chan L. Hybrid photovoltaic and thermal solar-collector designed for natural circulation of water. Appl Energy 2006;83:199–210.
[10] Tripanagnostopoulos Y. Aspects and improvements of hybrid photovoltaic/thermal solar energy systems. Sol Energy 2007;81:1117–31.
[11] Kalogirou SA, Tripanagnostopoulos Y. Hybrid PV/T solar systems for domestic hot water and electricity production. Energy Convers Manage 2006;47:3368–82.
[12] Erdil E, Ilkan M, Egelioglu F. An experimental study on energy generation with a photovoltaic (PV) – solar thermal hybrid system. Energy 2008;33:1241–5.
[13] Zondag HA, van Helden WGJ, Bakker M, Affolter P, Eisenmann W, Fechner H, et al. PVT Roadmap: A European guide for the development and market introduction of PVT technology. 20th European photovoltaic solar energy conference; 2005.
[14] Affolter P, Eisenmann W, Fechner H, Rommel M, Schaap A, Sørensen H, et al. PVT ROADMAP A European guide for the development and market introduction of PV-thermal technology; 2006.
[15] Huang BJ, Lin TH, Hung WC, Sun FS. Performance evaluation of solar photovoltaic/thermal systems. Sol Energy 2001;70:443–8.
[16] ENERGIES-SOL. Energie Solaire Photovoltaïque, Station Recharge Véhicules Electriques. <http://www.energies-sol.com/Files/45_ficha_tecnica__pvt.pdf> [accessed August 2012].
[17] Newform Energy. Newform Energy PVT Brochures. <http://www.newformenergy.com/pvt-downloads> [accessed March 2012].
[18] PVTWins. PVTWins hybrid systems. <http://www.pvtwins.nl/main01.html> [accessed March 2012].
[19] Millenium Electric. Millenium Electric PVT-250w-M-02 Data-sheet. <http://www.millenniumsolar.com/files/Products/Mil-PVT-250w-M-02-Data-sheet.pdf> [accessed March 2012].
[20] Zakharchenko R, Licea-Jimenez L, Perez-Garcia S, Vorobiev P, Dehesa-Carrasco U, Perez-Robles J, et al. Photovoltaic solar panel for a hybrid PV/thermal system. Solar Energy Mater Solar Cells 2004;82:253–61.
[21] Dubey S, Tiwari GN. Analysis of PV/T flat plate water collectors connected in series. Sol Energy 2009;83:1485–98.
[22] Zondag HA, de Vries DW, van Helden WGJ, van Zolingen RJC, van Steenhoven AA. The yield of different combined PV-thermal collector designs. Sol Energy 2003;74:253–69.
[23] Vokas G, Christandonis N, Skittides F. Hybrid photovoltaic–thermal systems for domestic heating and cooling—a theoretical approach. Sol Energy 2006;80:607–15.
[24] Zondag HA, De Vries DW, Van Helden WGJ, Van Zolingen RJC, Van Steenhoven AA. The thermal and electrical yield of a PV-thermal collector. Sol Energy 2002;72:113–28.
[25] Chow T, He W, Ji J. Hybrid photovoltaic-thermosyphon water heating system for residential application. Sol Energy 2006;80:298–306.
[26] Hobbi A, Siddiqui K. Optimal design of a forced circulation solar water heating system for a residential unit in cold climate using TRNSYS. Sol Energy 2009;83:700–14.
[27] Jordan U, Vajen K. Influence of the DHW load profile on the fractional energy savings: A case study of a solar combi-system with TRNSYS simulations. Sol Energy 2001;69(suppl. 6):197–208.
[28] Notton G, Cristofari C, Mattei M, Poggi P. Modelling of a double-glass photovoltaic module using finite differences. Appl Therm Eng 2005;25:2854–77.
[29] Kalogirou S. Solar thermal collectors and applications. Prog Energy Combust Sci 2004;30:231–95.
[30] Tiwari A, Sodha MS. Performance evaluation of solar PV/T system: An experimental validation. Sol Energy 2006;80:751–9.
[31] Kumar Agarwal R, Garg HP. Study of a photovoltaic-thermal system – thermosyphonic solar water heater combined with solar cells. Energy Convers Manage 1994;620.
[32] Cristofari C, Canaletti J, Notton G, Darras C. Innovative patented PV/TH Solar Collector: Optimization and performance evaluation. Energy Proc 2012;14:235–40.
[33] Duffie JA, Beckman WA. Solar energy thermal processes. New York; London: Wiley-Interscience; 1974.
[34] Incropera FP. Fundamentals of heat and mass transfer. 6th ed. Chichester, Hoboken, N.J., USA: Wiley, John Wiley; 2007.
[35] Lunde PJ. Solar thermal engineering: Space heating and hot water systems. New York; Chichester: Wiley; 1980.
[36] DECC. WindSpeed database: Department of energy and climate change. <http://www.decc.gov.uk/en/windspeed/default.aspx> [accessed March 2012].
[37] Skoplaki E, Palyvos JA. On the temperature dependence of photovoltaic module electrical performance: A review of efficiency/power correlations. Sol Energy 2009;83:614–24.
[38] Grundfos. The Centrifugal Pump 8/25/2012.
[39] Silió Salcines D, Renedo Estébanez C, Castañera Herrero V. Simulation of a solar domestic water heating system, with different collector efficiences and different volumen storage tanks 2010; 2012.
[40] Murphy GB, Kummert M, Anderson BR, Counsell J. A comparison of the UK standard assessment procedure (SAP) and detailed simulation of building-integrated renewable energy systems; 2009.
[41] Widén J, Wäckelgård E. A high-resolution stochastic model of domestic activity patterns and electricity demand. Appl Energy 2010;87:1880–92.
[42] Department for Communities and Local Government. House building – housing. <http://www.communities.gov.uk/housing/housingresearch/housingstatistics/housingstatisticsby/housebuilding/> [accessed March 2012].
[43] Department for Communities and Local Government. English Housing Survey (EHS) – housing. <http://www.communities.gov.uk/housing/housingresearch/housingsurveys/englishhousingsurvey/> [accessed March 2012].
[44] DECC Personal Communication. Average available roof area in a Terrace house in the UK; 2012.
[45] Richardson I, Thomson M, Infield D, Clifford C. Domestic electricity use: A high-resolution energy demand model. Energy Build 2010;42:1878–87.
[46] UKERC Energy Data Centre. Browse EDC archive. <http://data.ukedc.rl.ac.uk/browse/edc/Electricity/LoadProfile/data> [accessed March 2012].
[47] Wright A, Firth S. The nature of domestic electricity-loads and effects of time averaging on statistics and on-site generation calculations. Appl Energy 2007;84:389–403.
[48] Energy Saving Trust England. Measurement of domestic hot water consumption in dwellings/monitoring/housing professionals/publications/home (England); 2008.
[49] Suri M, Huld TA, Dunlop ED, Ossenbrink HA. Potential of solar electricity generation in the European Union member states and candidate countries. Sol Energy 2007;81:1295–305.
[50] Fritsch J. Heat pumps UK – world renewables 2010 – a multi client study. BSRIA 2011.
[51] BRECSU. Boiler efficiency database. <http://www.boilers.org.uk/> [accessed March 2012].
[52] Kensa Heat Pumps. Fact sheet – GSHP versus ASHP-01. 2009; 2012.
[53] Energy Saving Trust. Heat pumps in the UK – a monitoring report; 2005.
[54] Zondag HA. Flat-plate PV-Thermal collectors and systems: A review. Renew Sustain Energy Rev 2008;12:891–959.
[55] International Energy Agency. Technology roadmap. Solar photovoltaic energy; 2010.

[56] Cao S, Hasan A, Sirén K. Matching analysis for on-site hybrid renewable energy systems of office buildings with extended indices. Appl Energy 2014;113:230–47.
[57] Amori KE, Taqi Al-Najjar HM. Analysis of thermal and electrical performance of a hybrid (PV/T) air based solar collector for Iraq. Appl Energy 2012;98:384–95.
[58] Amrizal N, Chemisana D, Rosell JI. Hybrid photovoltaic–thermal solar collectors dynamic modeling. Appl Energy 2013;101:797–807.
[59] Bosanac M, Sørensen B, Katic I, Sørensen H, Nielsen B, Badran J. Photovoltaic/thermal solar collectors and their potential in Denmark; 2003.
[60] Santbergen R. Optical absorption factor of solar cells for PVT systems; 2008.
[61] Grundfos. Grundfos UK. <http://uk.grundfos.com/> [accessed August 2012].
[62] Kreith F, Goswami D. Handbook of energy efficiency and renewable energy. LLC: Taylor & Francis Group; 2007.